

Comparative Transduction Mechanisms of Hair Cells in the Bullfrog Utriculus. II. Sensitivity and Response Dynamics to Hair Bundle Displacement

4.6.01
p. 21

RICHARD A. BAIRD

Department of Neuro-otology and R. S. Dow Neurological Sciences Institute, Good Samaritan Hospital and Medical Center, Portland, Oregon 97209

SUMMARY AND CONCLUSIONS

1. Hair cells in whole-mount in vitro preparations of the utricular macula of the bullfrog (*Rana catesbeiana*) were selected according to their macular location and hair bundle morphology. The sensitivity and response dynamics of selected hair cells to natural stimulation were examined by recording their voltage responses to step and sinusoidal hair bundle displacements applied to their longest stereocilia.

2. The voltage responses of 31 hair cells to sinusoidal hair bundle displacements were characterized by their gains and phases, taken with respect to peak hair bundle displacement. The gains of Type B and Type C cells at both 0.5 and 5.0 Hz were markedly lower than those of Type F and Type E cells. Phases, with the exception of Type C cells, lagged hair bundle displacement at 0.5 Hz. Type C cells had phase leads of 25–40°. At 5.0 Hz, response phases in all cells were phase lagged with respect to those at 0.5 Hz. Type C cells had larger gains and smaller phase leads at 5.0 Hz than at 0.5 Hz, suggesting the presence of low-frequency adaptation.

3. Displacement-response curves, derived from the voltage responses to 5.0-Hz sinusoids, were sigmoidal in shape and asymmetrical, with the depolarizing response having a greater magnitude and saturating less abruptly than the hyperpolarizing response. When normalized to their largest displacement the linear ranges of these curves varied from <0.5 to 1.25 μm and were largest in Type B and smallest in Type F and Type E cells. Sensitivity, defined as the slope of the normalized displacement-response curve, was inversely correlated with linear range.

4. The contribution of geometric factors associated with the hair bundle to linear range and sensitivity were predicted from realistic models of utricular hair bundles created using morphological data obtained from light and electron microscopy. Three factors, including 1) the inverse ratio of the lengths of the kinocilium and longest stereocilia, representing the lever arm between kinociliary and stereociliary displacement; 2) tip link extension/linear displacement, largely a function of stereociliary height and separation; and 3) stereociliary number, an estimate of the number of transduction channels, were considered in this analysis. The first of these factors was quantitatively more important than the latter two factors and their total contribution was largest in Type B and Type C cells. Theoretical models were also used to calculate the relation between rotary and linear displacement. When expressed in terms of angular rotation, differences in sensitivity among hair cell types were increased, suggesting that these differences were not due to the manner in which hair bundles were stimulated in these studies.

5. The voltage responses of 16 hair cells to sinusoidal displacement were examined at four or more frequencies from 0.5 to 125 Hz. Type B and Type E cells had small bandwidths, with falling gains and increasing phase lags at all frequencies. In contrast, Type

C cells displayed 10- to 20-fold gain enhancements as frequency was increased and phase leads, ranging from 20 to 40°, were seen between 0.5 and 20 Hz. At higher frequencies, Type C cells had decreasing gains and increasing phase lags. Individual Type C cells displayed differing amounts of gain enhancement and phase lead at low frequencies. Rapidly adapting cells, distinguished by larger gain enhancements and larger phase leads, were more likely to be located in the outer striolar rows than slowly adapting cells. Type F cells did not adapt, displaying constant gains and near-zero phases at low frequencies.

6. Mean sinusoidal gains and phases to hair bundle displacement were fit by a transfer function, $H(s) = H_A(s) \cdot H_T(s)$, consisting of two terms thought to represent the adaptation associated with mechano-electrical transduction (H_A) and the gating kinetics of voltage-dependent membrane conductances (H_T). H_T was represented by a first- or second-order filter, with upper corner frequencies ranging from <1 to >50 Hz. H_A was best fit by a lead operator with a fractional exponent, k_A . At frequencies above an upper corner frequency ranging from <1 to 10 Hz, this operator introduced a gain that increased as f^{k_A} and a phase lead that approached $90^\circ \cdot k_A$. There was a systematic increase in this exponent from $k_A = 0$ for nonadapting hair cells to $k_A = 0.25\text{--}0.40$ for adapting hair cells.

7. The response dynamics of hair cells to hair bundle displacement differed in two respects from those to intracellular current. 1) hair cells that adapted to hair bundle displacement did not adapt to intracellular current. 2) the bandwidths of cells to hair bundle displacement were greater than those to intracellular current, presumably reflecting the increased conductance of transduction channels.

8. The response dynamics of 15 hair cells were examined with step hair bundle displacements. Type B cells in both the striolar and extrastriolar regions displayed little or no adaptation to step displacements. Other hair cell types displayed conspicuous response declines during step displacement and hyperpolarizing undershoots at their termination. The rate and extent of adaptation varied in different hair cell types. Type C cells, for example, were rapidly or slowly adapting, reaching steady-state levels in 50–100 ms or 100–200 ms, respectively. Type F and Type E cells adapted more slowly, reaching steady-state values in 300–500 ms. With the exception of Type E cells, rapidly adapting cells declined to a greater extent than slowly adapting cells.

9. With the possible exception of rapidly adapting Type C cells, the peak and steady-state responses of adapting hair cells were linearly related to step amplitude, suggesting that the time course and extent of adaptation were independent of displacement. The time course and extent of adaptation, however, were functions of step duration, suggesting that adaptation was activated at the onset of the step displacement but its kinetics were controlled by an intermediate process with variable response dynamics. This pro-

cess may reflect the kinetics of calcium regulation in different hair cell types.

10. These results indicate that hair cells in the utricular macula are organized to encode both static and dynamic information. This is largely accomplished by varying the rate and extent of adaptation in different hair cell types. Type B cells in both the striolar and extrastriolar regions are nonadapting. Hair cells restricted to the striolar region, on the other hand, adapt to maintained hair bundle displacement, with Type C cells adapting most rapidly and Type F and Type E cells adapting least rapidly. These results also suggest that utricular afferents derive much of their low-frequency response dynamics from the adaptation kinetics of their innervated hair cells. In particular, phasic-tonic afferents may derive tonic sensitivity from non-adapting and phasic sensitivity from adapting hair cells. Additional micromechanical factors, such as differences in the way in which individual hair cells couple to the otoconial membrane, may also be involved.

INTRODUCTION

The vertebrate utricle, one of the vestibular otolith organs, is a sensor of static gravity and dynamic linear acceleration (Lewis et al. 1982). In a companion study (Baird 1994) I studied the voltage responses of hair cells in the bullfrog utricle to intracellular current to understand how these receptor cells transduce both tonic and dynamic head and body movement. These studies were motivated by morphophysiological studies that have suggested that the diversity of physiological responses of utricular afferents is determined, at least in part, by regional variations in hair cell transduction mechanisms (Baird and Lewis 1986).

My companion studies revealed that hair cells in the bullfrog utricle, classifiable as Type II by cell body and synapse morphology (Wersall and Bagger-Sjoberg 1974), differ markedly in hair bundle morphology (Lewis and Li 1975). These hair cell types have unique macular distributions. Moreover, they differ in their passive and active membrane properties (Baird 1992, 1994), suggesting that they possess different basolateral membrane conductances. These basolateral conductances, by acting as frequency-dependent filters of the receptor current, can modify the responses of hair cells to natural stimulation, regulating sensitivity, frequency selectivity, and modulating synaptic release. My previous results suggest that the utricle is regionally organized, with hair cells in the central, or striolar, region of the utricle having faster outward potassium currents than hair cells in the peripheral, or extrastriolar, zone. Moreover, hair cells in the innermost striola, but no others, exhibit electrical resonance. This phenomenon, similar to that seen in some auditory (Crawford and Fettiplace 1981; Fuchs et al. 1988; Pitchford and Ashmore 1987) and vibratory (Ashmore 1983; Hudspeth and Lewis 1988; Lewis and Hudspeth 1983) hair cells, is known to sharpen frequency tuning.

In the present study, I was interested in seeing whether hair cell types in the bullfrog utricle might also differ in their voltage responses to hair bundle displacement. I was particularly interested in assessing the contributions of two factors to the responses of utricular hair cells. First, I was interested in examining the effect of hair bundle morphology on the sensitivity of hair cells to natural stimulation. This interest was motivated by the observation that vestibular

hair cells, unlike many auditory hair cells, are not free-standing but rather linked to an accessory cupular or otolithic membrane via the tip of their kinocilium (Hudspeth 1986; Roberts et al. 1988; Wersall and Bagger-Sjoberg 1974). Natural stimuli are initially transmitted to this accessory membrane, which in turn deflects the hair bundles of hair cells. This suggests that the morphology of the hair bundle is important for determining the sensitivities of individual hair cells to natural stimulation. I therefore used theoretical models of hair bundles to examine the contribution of geometric factors associated with these bundles to natural sensitivity in different hair cell types.

I was also interested in examining the contribution, if any, of adaptation to the response properties of utricular hair cells. As previous studies have shown, hair cells in auditory (Crawford et al. 1989, 1991) and vibratory (Assad and Corey 1992; Assad et al. 1989; Eatock et al. 1987; Hacohen et al. 1989) inner ear endorgans adapt to maintained displacements of their hair bundles, sharply limiting their low-frequency sensitivity. This adaptation is mediated by a shift in the displacement-response curve (DRC) of the hair cell along the displacement axis. Adaptation does not depend on the current through the transduction channel (Assad et al. 1989; Eatock et al. 1987). Moreover, adaptation of the receptor current proceeds when hair cells are voltage clamped to their resting membrane potential and so is not a consequence of the voltage change after hair bundle displacement. These observations suggest that the adaptation process occurs within the hair bundle and precedes mechanoelectric transduction. Recent observations of time-dependent changes in hair bundle stiffness are consistent with this conclusion (Howard and Hudspeth 1987, 1988).

Adaptation would be expected to be most useful in inner ear endorgans in which hair cells are subject to large static displacements that could potentially saturate their instantaneous response and compromise their sensitivity to high-frequency stimulation. Hair cells in these organs, by adapting to these static displacements, would restore their sensitivity to smaller, more dynamic stimuli. The adaptation process also permits hair cells to maintain their sensory hair bundle in the most sensitive portion of their DRC. In vestibular otolith organs in which static sensitivity is desirable, such as those endorgans that provide static gravitational sensitivity, any adaptation process in the hair cells may be undesirable. In these hair cells, the adaptive shift process may not exist or may proceed at a very low rate. To test this hypothesis, I measured the rate and extent of the decline of the voltage responses of utricular hair cells to step and sinusoidal hair bundle displacements. I then compared, for similar resting potentials and response amplitudes, the voltage responses of individual hair cells to both hair bundle displacement and intracellular current.

These results suggest that hair cells in the bullfrog utricle, besides differing in their basolateral membrane conductances, also differ in their sensitivity and response dynamics to hair bundle displacement. Sensitivity differences between hair cells are at least partially due to geometric factors associated with the stereociliary array. Differences in the low-frequency response dynamics of utricular hair cells, on the other hand, appear to largely reflect the time course of adaptation in individual hair cells. Moreover,

studies of the peripheral innervation patterns of utricular afferents (Baird and Schuff 1994) further suggest that the kinetics of the hair cell adaptation process also determine the tonic and phasic sensitivities of utricular afferents to head and body movement.

Preliminary accounts of portions of this data have been presented in both abstract (Baird and Schuff 1990, 1991) and short manuscript form (Baird 1992).

METHODS

Whole-mount *in vitro* preparations of the utricular macula were isolated as in the preceding paper (Baird 1994). Briefly, bisected utricular maculae were mounted flat, hair cells uppermost, within a small chamber on the fixed stage of an upright microscope (Zeiss model 16). I then positioned macular pieces so that the morphological polarization vectors of hair cells in the central macula were oriented perpendicular to a stimulating probe. The macular locations and hair bundle morphology of selected hair cells were identified on-line using Nomarski optics and a contrast-enhancement video camera (Hamamatsu C2400-07). Camera images of selected hair cells were stored on an S-VHS videotape recorder (Panasonic PV-S4864). The apical surfaces of selected utricular hair cells were impaled as in the previous paper (Baird 1994) with conventional intracellular microelectrodes pulled from thin-walled aluminosilicate glass.

Hair bundle stimulation

Hair cells were mechanically stimulated by deflecting their hair bundles with stiff borosilicate glass probes pulled to 0.5 to 1.0- μm tips (Corey and Hudspeth 1980). Stimulating probes were bent using a heated filament so that their final millimeter was parallel to the plane of the macula. After being cleaned in a sulfate-nitric acid solution and rinsed in distilled water they were mounted to a piezoelectric bimorph element (Vernitron PZT-5B) and driven via leads soldered to their nickel-plated surface by a waveform generator (Wavetek model 185). The driving signal from this generator was filtered at 1 kHz to minimize a probe mechanical resonance at ~ 10 kHz. Stimulating probes were positioned against the hair bundle of selected hair cells with a hydraulically controlled Huxley-style micromanipulator (Sutter). Probe motion in response to applied voltages was calibrated against a stage micrometer at high magnification ($\times 10,000$).

I had originally hoped to stimulate hair cells at the distal tip of their kinocilium to simulate the action of natural stimulation on the hair bundle. It proved difficult, however, to visualize and couple stimulating probes to the distal tip of the kinocilium in whole-mount preparations. Hair cells were therefore approached from the stereociliary side and stimulated at the level of their longest stereocilia. After coupling the stimulus probe to the hair bundle I made small adjustments of the stimulating probe with the Huxley-style micromanipulator or by adjusting a DC bias voltage applied to the stimulating probe. The probe position that gave the largest voltage response to a 5.0-Hz sinusoidal stimulus was taken as the resting position of the hair bundle. Stimulus probes were observed on a video monitor at high magnification ($\times 10,000$) during hair bundle displacement to verify the lack of relative motion between the probe and the hair bundle. Theoretical models of hair bundles were used to normalize the resulting responses for differences in hair bundle morphology (see below).

Data analysis

Sinusoidal hair bundle displacements at 0.5 or 5.0 Hz, presented in bursts of five to six cycles, were delivered to hair cells via stimulating probes. The amplitude of sinusoidal hair bundle dis-

placements was varied from 0.25 to 2 μm , producing peak voltage responses from <5 to 20 mV. Setting the stimulus amplitude to give a maximum response at <10 mV, I then examined the responses of hair cells to sinusoidal hair bundle displacements in the frequency range from 0.5 to 200 Hz using individual sinusoids and logarithmic frequency sweeps. If possible the responses of hair cells to sinusoidal intracellular current were also recorded. During frequency sweeps hair cells were stimulated at a start frequency (0.5 or 5.0 Hz) for several seconds before initiation of the frequency sweep. They were then stimulated successively for ~ 1 s each with 15 additional frequencies (not including the end frequency) equally spaced in frequency from the start frequency (0.5 or 5.0 Hz) to the end frequency (20 or 200 Hz). For both stimuli the responses to successive sine wave cycles were averaged; the number of averaged cycles varied with stimulus frequency, ranging from 2 at 0.5 Hz to 16 at 125 Hz. Sinusoidal gains and phases were extracted by a Fourier analysis of the averaged responses and expressed with respect to peak intracellular current or hair bundle displacement. Gain was calculated as the ratio of a hair cell's response amplitude at the fundamental frequency divided by the amplitude of intracellular current or hair bundle displacement. Nonlinear distortion was measured as the ratio of the root-mean-squared (rms) amplitude of the second to the fifth harmonics to the rms amplitude of the fundamental component.

The response dynamics of hair cells to hair bundle displacement were further assessed with step displacements of varying amplitude and duration, displacing the hair bundle both parallel and antiparallel to its vector of morphological polarization. Step displacements (100 ms to 10 s in duration) were usually alternated between positive (excitatory) and negative (inhibitory) values, starting at 1 or 2 μm and halving step amplitude with each iteration until reaching a final value of 0.25 μm . In a few cases the stimulating probe was visually observed to lose contact with the hair bundle during the return phase of a step displacement. This loss of contact was correlated with a slow return of membrane potential to its resting value rather than a distinct discontinuity at the termination of the displacement step.

Calculational procedures

DRCs. DRCs were determined from the rising or falling phases of the response to 5.0-Hz sinusoidal hair bundle displacements by plotting, for each cycle of the sinusoidal stimulus, the value of membrane voltage versus hair bundle displacement. The intersection of the DRCs derived from the rising and falling phases of the sinusoidal responses was taken to be the rest position of the hair bundle. To minimize the phase shift and hysteresis associated with the sinusoidal stimulus I then shifted the DRC derived from the rising phase of the sinusoidal response with respect to the displacement axis to place the rest position at zero displacement and normalized the result to its maximum voltage response. Normalized DRCs derived from the rising phases of the sinusoidal responses of individual cells were then averaged to obtain the mean DRCs of different hair cell types. The linear range of DRCs was defined to be the range of displacements that generated 10–90% of the normalized voltage response. Sensitivity of a hair cell to displacement was defined as the slope of its normalized DRC within its linear range.

TRANSFER FUNCTIONS. A nonlinear modeling technique was used to fit a transfer function, $H(s)$, the ratio of the Laplace transform of the voltage response to the Laplace transform of the sinusoidal stimulus, to a set of mean frequency response data given by gain and phase values at specified discrete frequencies (Seidel 1975). The general form and number of parameters of a transfer function, $H(s)$, were first specified in terms of a gain term, any number of simple or complex poles and/or zeros, and, if desired, a zero term raised to a fractional exponent. A Fortran computer

program (TRNFIT) then provided estimates of the fit parameters on the basis of a minimization of the squared error between the fit model and the mean gain and phase data. This error was weighted by the difference in frequency between succeeding data points and taken over all frequencies for which mean data was available. Fits provided by transfer functions were described in terms of rms errors in gain and phase.

Morphological analyses

To examine the hair bundle morphology of individual utricular hair cells in detail, two utricular maculae were prepared for electron microscopy. Maculae were first fixed for 2 h in a solution containing 1.25% glutaraldehyde-1.0% paraformaldehyde and 5 mM CaCl_2 in 0.1 M phosphate buffer (pH 7.25). They were then postfixed at 4°C for 1 h in a 1.0% glutaraldehyde-1.0% osmium tetroxide solution in 0.1 M phosphate buffer, dehydrated in a series of ethanol solutions, and embedded in acrylic resin (London Resin LR White). After embedding, the hair bundles of hair cells were serially sectioned at a thickness of 200 nm on an ultramicrotome (LKB Nova). Thin sections were collected on Formvar-coated grids and stained for 3 min with 10% uranyl acetate in 25% ethanol and 10–20 s with lead citrate. Thick (0.2 μm) sections were cut every 1 μm to ensure the completeness of the hair bundle, to determine the position of thin sections from the apical surface, and to allow individual hair bundles to be identified at the light microscopic level. Thin sections were examined, photographed, and videotaped in a transmitting electron microscope (Zeiss 10C/A) operated at an accelerating voltage of 80 kV.

Hair cells were identified, as in previous studies (Baird 1992, 1994), from their macular location and hair bundle morphology. This was done by examining thick sections of hair bundles at varying heights above the apical surface and noting the size of the hair bundle, the presence or absence of a bulbous kinocilium, and the relative lengths of the kinocilium and longest stereocilia. Selected hair bundles were then further examined in thin sections taken above the height of the apical surface and below the height of their shortest stereocilia. Splayed hair bundles were excluded from further analysis.

Electron photomicrographs and videotaped images of selected hair bundles were input to a computerized image analysis system (Bioquant System IV) for morphometric analysis (Fig. 1, *a* and *b*). For each identified hair bundle the number of stereocilia were counted. Mean stereociliary diameter was determined by averaging the diameter of all stereocilia in the stereociliary array. The mean spacing between adjacent stereocilia was determined by averaging the distance between stereocilia in adjacent rows.

Theoretical models of utricular hair bundles

Theoretical models of utricular hair bundles were created using morphological data from our electron microscopic studies and the previous paper (Baird 1994). I first estimated the relation between angular rotation and linear displacement for different hair cell types, assuming that the stereociliary array pivoted as a stiff beam about its base. Using simple geometry (Fig. 1*c*), the angle of rotation, Θ_r , is equal to $\sin^{-1}(x/l_s)$, where x is the linear displacement applied to the hair bundle and l_s is the length of the longest stereocilia (Table 1, Baird 1994).

The hair bundles of individual hair cell types were further characterized by three geometric factors, the product of which represents the total contribution of these factors to hair cell sensitivity. The first factor was a measure of the mechanical advantage afforded the hair bundle by the differential anchoring points of its kinocilium and longest stereocilia (Fig. 1*c*). This factor was determined from the ratio of the lengths of the kinocilium (l_k) and the

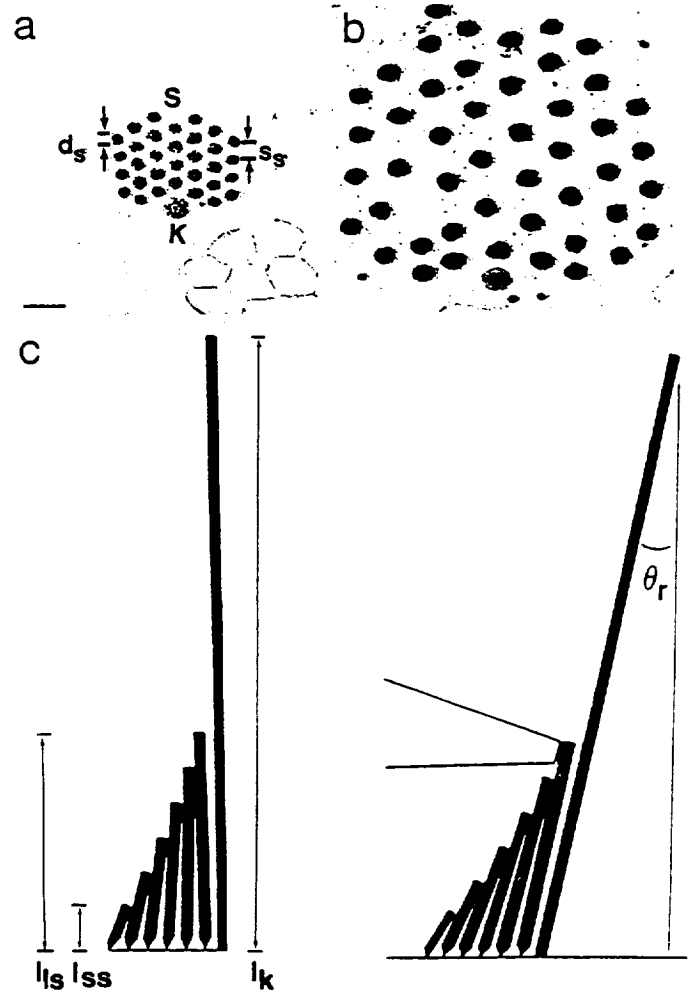


FIG. 1. Transmission electron photomicrographs of cross-sectioned Type B (*a*) and Type F (*b*) hair bundles in the medial extrastricular and striolar regions, respectively. *c*: schematic representation of hair bundle during excitatory displacement with definition of geometric variables used in theoretical modeling. K, kinocilium; l_k , kinociliary length; S, stereocilia; l_s , longest stereociliary length; l_{ss} , shortest stereociliary length; d_s , stereociliary diameter; s_s , stereociliary spacing; Θ_r , angular rotation. Bar: 1 μm .

longest stereocilia (l_s), mean values of which were obtained from the previous paper (Table 1, Baird 1994). A second factor, expressed as the amount of tip-link extension per linear displacement, was calculated using BUNDLE, a computer program created by Dr. D. Corey of the Massachusetts Eye and Ear Infirmary. In this calculation, the length, diameter, and spacing of individual stereocilia in different hair cell types were obtained from my electron microscopic studies. The resting position and resting lengths of tip links were arbitrarily assigned to typical values for saccular hair cells (D. Corey, personal communication). The third factor, a measure of the number of transduction channels, was set equal to 5 times the number of stereocilia in the hair bundle (Holton and Hudspeth 1986).

Statistical procedures

Unless otherwise stated, statistical comparisons of morphometric and physiological data were based on a one-way analysis of variance. Where appropriate, post hoc pairwise multiple comparisons were performed using the Tukey multiple comparison test, adjusting when necessary for unequal group sizes (Miller 1977).

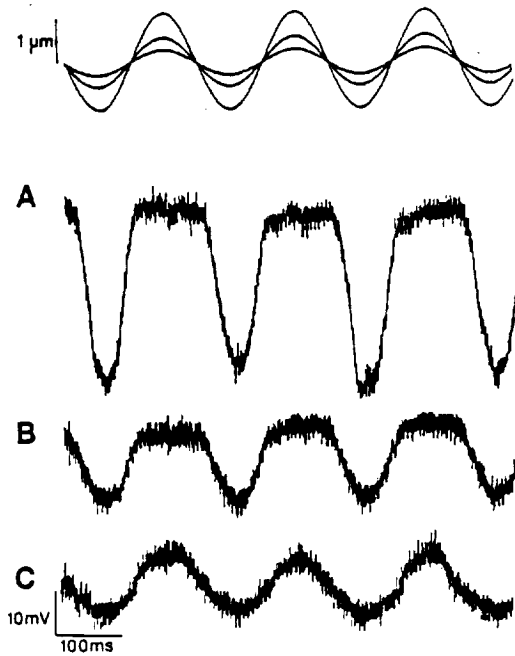


FIG. 2. Voltage responses of a Type F cell to 1.0- μm (A), 0.5- μm (B), and 0.25- μm (C) 5.0-Hz hair bundle displacements.

RESULTS

Responses to sinusoidal hair bundle displacement

The responses of 31 utricular hair cells were examined to 0.5- or 5.0-Hz sinusoidal hair bundle displacements. Of this total, 3 were Type B hair cells located in the medial extrastriola. The remaining 28 hair cells, including 4 Type B, 13 Type C, 7 Type F, and 4 Type E cells, were from the striolar region. I did not obtain the responses of any Type B cells in the lateral extrastriola to hair bundle displacement. The responses of hair cells to sinusoidal hair bundle displacements were characterized by their gains and phases, taken with respect to peak hair bundle displacement. Sinusoidal responses, even in the most sensitive hair cells, were linear for peak response amplitudes <10 mV (Fig. 2C), but become increasingly nonlinear for larger stimulus amplitudes (Fig. 2, A and B). At small stimulus amplitudes nonlinear distortion was usually near 10%. Response linearity was also studied in 10 cells by varying the amplitude of 5.0-Hz sinusoids from 0.25 to 1.0 μm . The variation of sinusoidal gain and phase with amplitude was small, averaging $\pm 10\%$ and $\pm 5^\circ$, respectively.

The sinusoidal gains and phases of 17 hair cells at 0.5 Hz and 31 hair cells at 5.0 Hz are plotted in Fig. 3, A and B, respectively. The gains of Type B cells, whether in the extrastricular (open circles) or striolar (solid circles) region, were markedly lower than those of other hair cell types (Fig. 3, A and B). This was also true, to a lesser extent, for Type C cells (squares). Type C cells also had large phase leads at 0.5 Hz. The phases of other cells, with the exception of two transitional cells (see below), lagged hair bundle displacement. Type B cells in the striola were more phase lagged than their extrastricular counterparts. Three hair cells (circled symbols) had transitional responses. These included a Type B cell that, like Type C cells, strongly phase-led hair bundle displacement and a Type C cell that, like Type B

cells, phase-lagged hair bundle displacement. Both these cells were located on the striolar border. In addition, one Type F cell had high gains but, like Type C cells, phase-led hair bundle displacement at both 0.5 and 5.0 Hz.

With the exception of Type C cells, gains at 5.0 Hz were less than or equal to those at 0.5 Hz. The responses of all hair cells were also more phase lagged at 5.0 than at 0.5 Hz. This is evident from Fig. 3C, which plots the gain ratio and

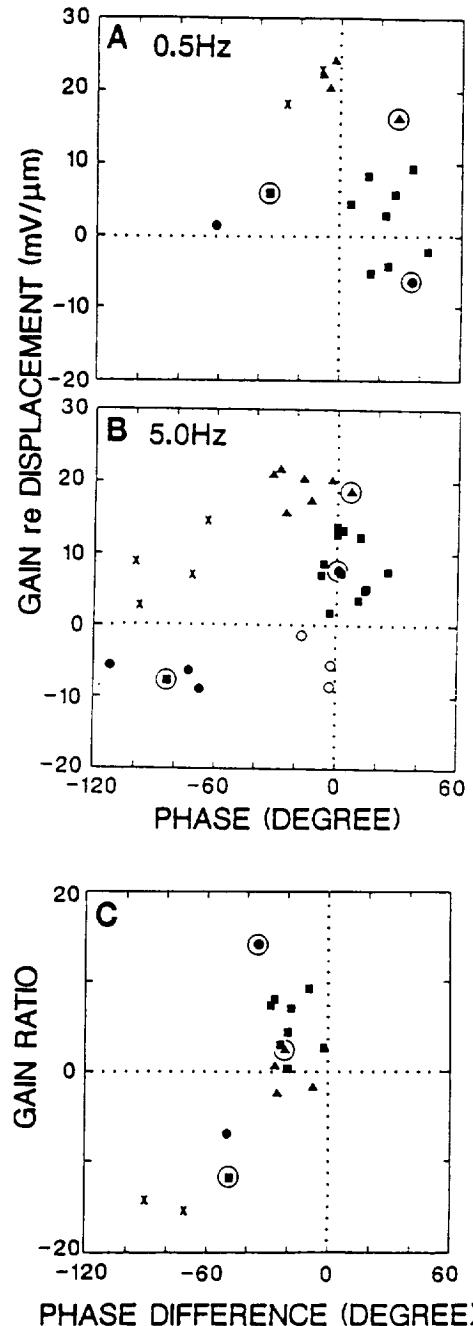


FIG. 3. A and B: gain plotted vs. phase for 17 hair cells at 0.5 Hz (A) and 31 hair cells at 5.0 Hz (B) in response to sinusoidal hair bundle displacement. C: gain ratio and phase difference between voltage responses at 5.0 and 0.5 Hz for 17 hair cells in A recorded to both 0.5- and 5.0-Hz sinusoidal hair bundle displacements. Extrastricular and striolar cells are represented by open and solid symbols, respectively. Circled symbols: 3 transitional hair cells with intermediate response properties (see text). Circles: Type B. Squares: Type C. Triangles: Type F. Crosses: Type E.

phase difference at 0.5 and 5.0 Hz for 17 cells that were examined at both frequencies. Type B (circles) and Type E (crosses) cells had smaller gains and larger phase lags at 5.0 Hz than at 0.5 Hz, suggesting that they had smaller bandwidths than other hair cell types. By contrast, the responses of Type C cells (squares) at 5.0 Hz were larger than at 0.5 Hz, indicating the presence of low-frequency adaptation (see below). The gains and phases of Type F cells (triangles) were similar at both frequencies.

DRCs of hair cells

DRCs, determined from the rising phase of the voltage responses of hair cells to 5.0-Hz sinusoids (see METHODS), were sigmoidal in shape. They were also asymmetrical, with their resting bundle position displaced toward negative displacements and the positive response evoked by movements toward the kinocilium exhibiting a greater magnitude and more gradual saturating approach than the negative response. When normalized to their largest displacement, these curves differed in both their linear range and their sensitivity to hair bundle displacement. Type B cells, in both the striolar (open circles) ($n = 2$) and medial extrastriolar (solid circles) ($n = 1$) regions, had the largest linear ranges of utricular hair cells (Fig. 4, *top*). Type C cells ($n = 8$) had somewhat smaller linear ranges, averaging $0.75 \mu\text{m}$ (Fig. 4, *top middle*). The linear ranges of Type F ($n = 6$) and Type E ($n = 3$) cells (Fig. 4, *bottom middle* and *bottom*), with the exception of a single transitional Type F cell (open triangles), were $<0.50 \mu\text{m}$ and were significantly smaller than those of Type B and Type C cells. The DRC of the transitional Type F cell closely resembled that of Type C cells. Sensitivity, defined as the slope of the normalized DRC, ranged from <0.50 to $>1.5 \mu\text{m}^{-1}$ and was inversely correlated with linear range.

Theoretical models of hair bundles

Differences in linear range and sensitivity between utricular hair cell types could be due to geometric factors associated with their hair bundles and to the way in which hair bundles were stimulated in this study. To test these possibilities, I created theoretical models of hair bundles using morphological data obtained from light and electron microscopy. These models were used to estimate the in situ sensitivities of different hair cell types and to quantify geometric factors associated with hair bundle types that might be involved in determining the sensitivity of individual hair cells to natural stimulation.

Morphometric data obtained from light and electron microscopy are summarized in Table 1, which also includes the results of statistical tests. Measurements of kinociliary and stereociliary lengths were determined from a morphological study of 135 hair cells in the previous paper (Baird 1994). The mean number, diameter, and spacing of stereocilia in the hair bundle of each hair cell type were measured in a separate population of 88 hair cells whose cross-sectioned hair bundles were examined in the electron microscope. When Type B and Type C cells are compared with Type F and Type E cells, the kinocilia of the former are longer and the shortest and longest stereocilia shorter in length than those of the latter. The stereocilia of Type B and

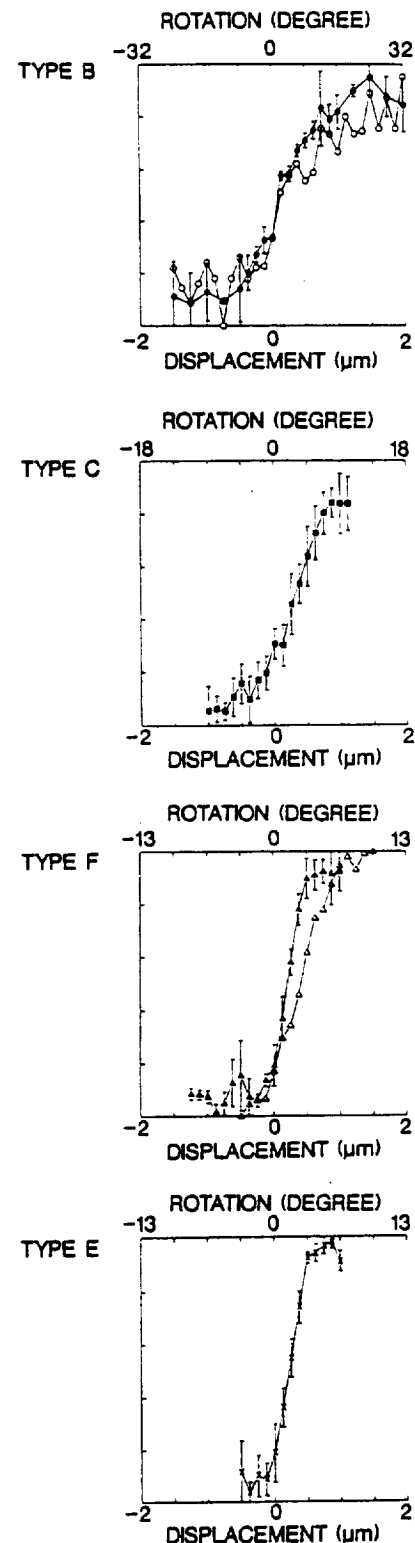


FIG. 4. Mean displacement-response curves (DRCs) of 3 Type B, 8 Type C, 6 Type F, and 3 Type E hair cells determined from the normalized voltage responses to 5.0-Hz hair bundle displacement. For Type B cells, open symbols indicate the DRC of an extrastriolar Type B cell; solid symbols indicate the mean DRC of two striolar Type B cells. For Type F cells, open symbols indicate the DRC of a transitional Type F cell whose voltage response, unlike those of typical Type F cells, demonstrated adaptation to hair bundle displacement (see text); solid symbols indicate the mean DRC of 5 typical Type F cells. Circles: Type B. Squares: Type C. Triangles: Type F. Crosses: Type E. Points: means. Bars: SDs.

TABLE 1. Morphological properties, utricular hair bundles

Cell Type	n	Stereociliary						
		Number	Diameter, μm	Spacing, μm	n	Shortest length, μm	Longest length, μm	Kinociliary Length, μm
Type B	22	38.0 \pm 3.9	0.19 \pm 0.03	0.33 \pm 0.04	55	1.1 \pm 0.5	3.8 \pm 1.0	12.2 \pm 1.9
MES	11	39.2 \pm 4.6	0.20 \pm 0.04	0.33 \pm 0.05	30	1.2 \pm 0.5	4.0 \pm 0.9	12.6 \pm 1.6
MS/LS	0	—	—	—	6	0.7 \pm 0.4	2.8 \pm 0.4	10.3 \pm 1.9
LES	11	36.8 \pm 3.0	0.17 \pm 0.01	0.32 \pm 0.04	19	1.1 \pm 0.4	3.9 \pm 1.0	12.1 \pm 2.0
Type C	15	42.4 \pm 6.0	0.24 \pm 0.04	0.38 \pm 0.06	41	1.3 \pm 0.6	6.3 \pm 1.2	16.6 \pm 2.3
Type F	32	46.7 \pm 5.9	0.33 \pm 0.05	0.70 \pm 0.08	23	1.9 \pm 0.9	8.2 \pm 1.3	9.3 \pm 1.2
Type E	19	34.7 \pm 6.3	0.33 \pm 0.05	0.69 \pm 0.08	16	2.1 \pm 0.7	8.9 \pm 1.1	9.8 \pm 1.1

Values are means \pm SD. *n* is number of hair bundles (left) or hair cells (right). Stereociliary number, diameter, and spacing were measured from electron micrographs of identified hair bundles. Kinociliary and stereociliary lengths were measured with light microscopy in a separate population of cross-sectioned hair cells (Baird 1994, Table 1). The following differences were statistically significant. Stereociliary number: Type F vs. Types B and E, Type C vs. Type E, $P < 0.001$. Stereociliary diameter: Types F and E vs. Types C and B, $P < 0.001$ in all cases. Stereociliary spacing: Types F and E vs. Types C and B, $P < 0.001$ in all cases; Type C vs. Type B, $P < 0.01$. Shortest stereociliary length: Type E vs. Types C and B, Type F vs. Type B, $P < 0.001$; Type F vs. Type C, $P < 0.005$. Longest stereociliary length: Types E and F vs. Types C and B, Type C vs. Type B, $P < 0.001$ in all cases. Kinociliary length: Types C and B vs. Types E and F, Type C vs. Type B, $P < 0.001$ in all cases. MES, medial extrastriola; MS, medial striola; LS, lateral striola; LES, lateral extrastriola.

Type C cells are also smaller in diameter and more closely spaced than those of Type F and Type E cells. Type F cells had greater numbers of stereocilia than other hair cell types. Regional variations in hair bundle morphology were small and insignificant.

Previous studies (Ohmori 1985, 1987) have argued that angular rotation, rather than lateral displacement, is the natural stimulus to hair cells. For technical reasons hair cells in this study were stimulated at the height of their longest stereocilia. Because this height varies for different hair cell types (Table 1) the rotary stimulus applied to hair cells was a function of stereociliary height. Using simple geometry I therefore calculated the relation between linear displacement and angular rotation to normalize the sensitivities of different hair cell types (Table 2). Assuming that each stereocilia pivots as a stiff beam about its base, the angular rotation experienced by the hair bundle, Θ_r , is equal to $\sin^{-1}(x/l_s)$, where x is the linear displacement applied to the hair bundle and l_s is the length of the longest stereocilia (Fig. 1C). Normalized sensitivities, expressed as a function of angular rotation, were markedly different in different hair cell types, with Type B, and to a lesser extent,

Type C cells having lower sensitivities to sinusoidal hair bundle displacement than Type F and Type E cells. Differences in the sensitivities of hair cell types were greatly enhanced by the normalization procedure, suggesting that differences in sensitivity between hair cell types were not due merely to the manner in which hair bundles were stimulated in these studies.

Hair bundles were also characterized by three geometric factors, the product of which represents the total contribution of these factors to hair cell sensitivity. These factors are summarized in Table 2, which also includes the results of statistical tests. The first factor, determined from the ratio of the lengths of the kinocilium and longest stereocilia, was a measure of the mechanical advantage afforded hair bundles by the differential anchoring points of their kinocilium and longest stereocilia. In this analysis I assumed that hair bundles were firmly attached to the otolith membrane by a rigid kinocilium and that displacement was conveyed to the stereociliary array via lateral linkages that attach the tallest stereocilia to the kinocilium. Under these circumstances the kinocilium would be expected to decrease the amplitude of the linear displacement experienced by the stereociliary

TABLE 2. Normalization factors, utricular hair bundles

Cell Type	n	Rotary/Lateral Displacement, $^\circ/\mu\text{m}$	Length Ratio, F1	n	Tip-link Extension/Lateral Displacement, F2	Number of Stereocilia, F3	Total, F1 \times F2 \times F3
Type B	55	16.4 \pm 5.0	0.32 \pm 0.08	22	0.092 \pm 0.029	38.0 \pm 3.9	1.07
MES	30	15.5 \pm 4.1	0.32 \pm 0.08	11	0.086 \pm 0.022	39.2 \pm 4.6	1.08
MS/LS	6	21.4 \pm 3.6	0.28 \pm 0.06	—	—	—	—
LES	19	16.2 \pm 5.8	0.33 \pm 0.08	11	0.090 \pm 0.032	36.8 \pm 3.0	1.09
Type C	41	9.5 \pm 1.9	0.38 \pm 0.07	15	0.062 \pm 0.014	42.4 \pm 6.0	1.18
Type F	23	7.2 \pm 1.1	0.89 \pm 0.10	32	0.087 \pm 0.017	46.7 \pm 5.9	3.62
Type E	16	6.5 \pm 0.8	0.92 \pm 0.12	19	0.076 \pm 0.010	34.7 \pm 6.3	2.43

Values are means \pm SD. *n* is number of hair cells (left) or hair bundles (right). Length into (F1) is the inverse ratio of the kinociliary and longest stereociliary lengths, obtained from the previous paper (Baird 1994, Table 1). Rotary/linear displacement is defined by $\sin^{-1}(x/l_s)$, where l_s is the length of the longest stereocilia. Stereociliary number, diameter, and spacing were measured from electron micrographs of identified hair bundles. Tip-link extension/lateral displacement (F2) is obtained from the above measurements and the computer program BUNDLE (see text). The following differences were statistically significant. Rotary/lateral displacement: Type B vs. Types C, F, and E, striolar Type B vs. MES Type B, $P < 0.001$; striolar Type B vs. LES Type B, $P < 0.01$; Type C vs. Types F and E, $P < 0.05$. Length ratio (F1): Types E and F vs. Types C and B, Type C vs. Type B, $P < 0.001$ in all cases. Tip link extension/lateral displacement (F2): Types B and F vs. Type C, $P < 0.001$; Type B vs. Type E, $P < 0.05$. Number of stereocilia (F3): Type F vs. Types B and E, Type C vs. Type E, $P < 0.001$. For abbreviations, see Table 1.

array and the in situ sensitivity of a hair cell would actually be less than that measured in this study. This reduction, which ranged in value from 0.16 to 1.08, was 2–3 times larger in Type B and Type C cells than in Type F and Type E cells (Table 2). A second factor, a measure of tip-link extension per linear stereociliary displacement, was calculated assuming that the hair bundle was stimulated at its longest stereocilia and that each stereocilia pivoted as a stiff beam about its base. This factor, which was largely dependent on the height and spacing of adjacent stereocilia in the stereociliary array, ranged in value from 0.04 to 0.18 and was larger in Type B and Type F cells than in Type C and Type E cells. Finally, I considered the possibility that hair bundles differed in their number of stereocilia and therefore the number of their transducer channels. The number of stereocilia in individual hair cells varied by a factor of two, ranging from 24 to 57. The mean number of stereocilia was significantly larger in Type F cells than in other hair cell types. On the basis of geometric factors alone, the above analysis suggests that Type B and Type C cells should have sensitivities to linear displacement 2–3 times smaller than those of Type F and Type E cells. This difference was due largely to the large mechanical advantage afforded Type F and Type E cells by their short kinocilium and long stereocilia.

Response dynamics to sinusoidal hair bundle displacements

The responses of 16 hair cells, including 2 Type B, 8 Type C, 3 Type F, and 3 Type E cells, were obtained to logarithmic sweeps of hair bundle displacement between 0.5 and 200 Hz (Fig. 5). There were striking differences in the responses of hair cells to sinusoidal hair bundle displacement. The responses of Type B cells were small and decreased sharply with increasing frequency. Type C cells had larger responses and responded to much higher frequencies than Type B cells. In addition, the responses of Type C cells showed conspicuous response declines for frequencies <5 Hz. Type F and Type E cells displayed the largest responses to hair bundle displacement. Type F cells had responses similar to those of Type C cells but did not exhibit response declines at low frequency. The responses of Type E cells declined sharply with increasing frequency, resembling the responses of Type B cells. At higher stimulus amplitudes these hair cells were also strongly rectifying, displaying a marked DC response at higher frequencies for which no fundamental response was evident. This rectification, unlike the low-frequency response declines in Type C cells (see below), was also evident in the responses of Type E cells to intracellular current (Baird 1994).

The effect of stimulus amplitude on sinusoidal gain and phase was not systematically examined at all stimulus frequencies. Rather, stimulus amplitude was adjusted between 0.5 and 2 μm to give a maximum response at <10 mV, a level of response for which the variation of sinusoidal gain and phase with stimulus amplitude at 5.0 Hz was small (Fig. 2). A similar result was seen in two Type C cells in which sinusoidal gain and phase were examined at multiple stimulus amplitudes at additional frequencies, justifying the presentation of frequency response data in the form of normalized Bode plots.

Bode plots for 16 individual hair cells for which voltage responses were obtained at four or more frequencies between 0.5 and 125 Hz are shown as solid lines in Fig. 6. Where applicable, the group means for the four hair cell types, separately calculated for gains and phases, are also shown (open circles). The responses of two Type B cells, one from the striola and the other from the medial extrastriola, are shown at the far left. For frequencies >5 Hz the extrastriolar Type B cell displayed falling gains and increasing phase lags with increasing frequency. The response of this cell was not examined at lower frequencies. The striolar Type B cell had a smaller bandwidth than its extrastriolar counterpart. In contrast, Type C cells displayed 10- to 20-fold gain enhancements as frequency was increased and phase leads, ranging from 20 to 40°, were seen between 0.5 and 20 Hz. At higher frequencies Type C cells displayed decreasing gains and increasing phase lags. Individual Type C cells displayed differing amounts of gain enhancement and phase lead at low frequencies. For higher frequencies the response dynamics of individual Type C cells were similar, suggesting that the response dynamics of Type C cells were governed by two components, one dominating their responses at lower frequency and the other dominating at higher frequencies (see below). Rapidly adapting Type C cells (heavy lines), distinguished by large gain enhancements and large phase leads, differed from more slowly adapting Type C cells (light lines) in two respects. 1) they had higher sensitivities to hair bundle displacement. 2) they displayed gain enhancements and phase leads at higher frequencies than more slowly adapting Type C cells. The degree of adaptation in Type C cells was also correlated with macular location, with rapidly adapting cells tending to be located in the outer striolar rows and slowly adapting cells in the inner striolar rows. In particular, two of three rapidly adapting Type C cells were located in the outer rows, whereas three of five slowly adapting Type C cells were located in the inner rows. Type F cells, with one prominent exception (heavy lines), had near-constant gains and phases hovering near zero at low frequencies. The exceptional cell, like Type C cells, displayed increasing gain and phase leads at low frequencies and, unlike typical Type F cells, was located in the outer striolar rows. At higher frequencies, Type F cells displayed decreasing gains and increasing phase lags. Type E cells had small bandwidths, displaying falling gains and increasing phase lags with increasing frequency.

Transfer functions

The gains and phases of individual Type B cells and the group means and phases of the hair cell types to hair bundle displacement were fit by a transfer function, $H(s) = H_A(s) \cdot H_T(s)$, made up of two components. As I will argue in the DISCUSSION, it is convenient to think of $H_A(s)$ as reflecting the dynamics of an adaptation process associated with mechanoelectric transduction and $H_T(s)$ as a dynamic component introduced by other transduction processes within the hair cell, primarily the gating kinetics of voltage-dependent conductances in the apical and basolateral membrane.

The response dynamics of adapting hair cells could not

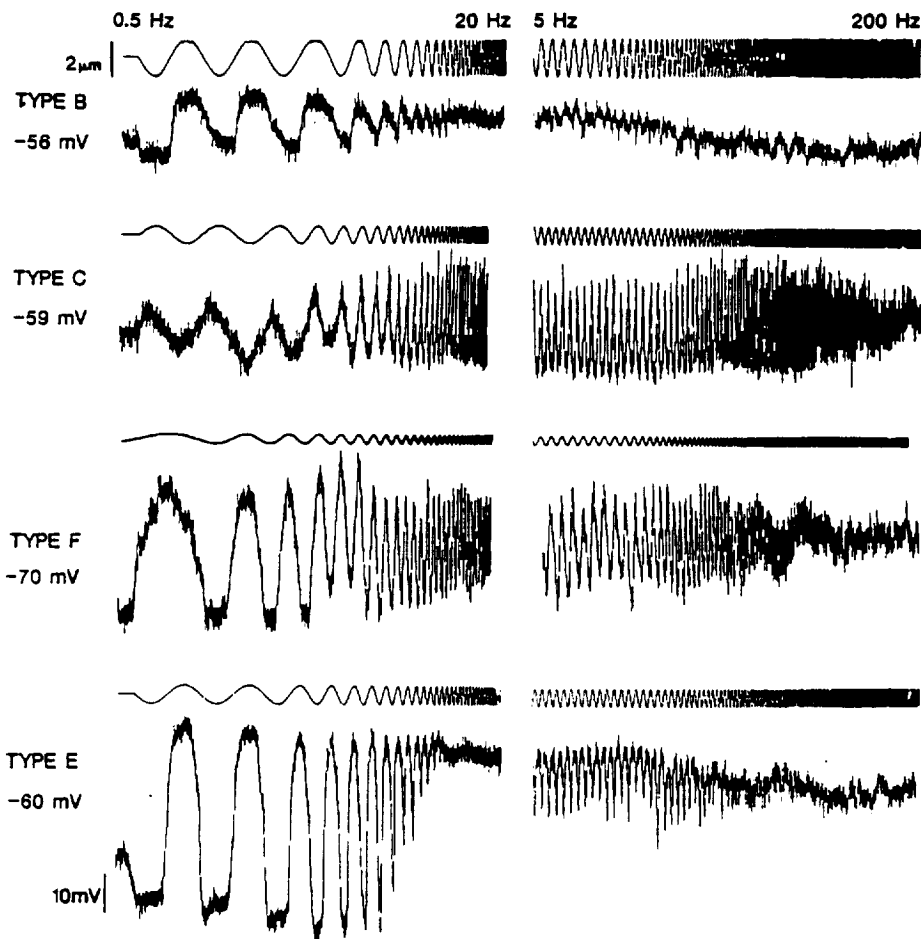


FIG. 5. Voltage responses of typical Type B, Type C, Type F, and Type E cells to logarithmic sweeps of sinusoidal hair bundle displacement in the frequency ranges of 0.5–20 and 5–200 Hz.

be fit by an integral lead operator because low-frequency gains in these cells increased as a fractional power of sinusoidal frequency and phase leads, even in the most rapidly adapting hair cells, did not approach 90° . I therefore adopted the first-order fractional-lead operator, $H_A(s) = (1 + s\tau_A)^{k_A}$, where k_A is a fractional exponent and τ_A is an adaptation time constant, to provide the gain enhancement and phase leads seen in adapting hair cells. This operator, above an upper corner frequency of $1/(2\pi\tau_A)$, introduces a gain that increases as f^{k_A} and a phase lead that approaches $90^\circ \cdot k_A$ (Thorson and Biederman-Thorson 1974). The high-frequency response dynamics of utricular hair cells were represented by a second-order lag element, $H_T(s) = 1/(1 + s\tau_{T1})(1 + s\tau_{T2})$, where τ_{T1} and τ_{T2} are time constants, because the phase lags of many cells at these frequencies were $>90^\circ$. This lag element accounts for the high-frequency phase lags observed in all hair cells and for the fact that the high-frequency phase leads seen in adapting hair cells were smaller than would be predicted solely from the fractional-lead operator.

The mean frequency response data of each hair cell type, illustrated in Fig. 7, was fit to the transfer function $H(s) = H_A(s) \cdot H_T(s)$ using a least-squares fit (see METHODS). The best-fitting transfer functions for each hair cell type in the frequency range from 0.5 to 125 Hz, shown as solid lines in Fig. 7, provided good approximations to the experimental data. The average gain and phase errors for all 16 hair cells were 9.5% and 3.7° , respectively. The small size of the fit-

ting errors implies that the Bode plots for the mean frequency response data can be summarized in terms of their transfer function parameters. The best-fitting transfer function parameters for the different hair cell types are summarized in Table 3. Type B and Type F cells (Fig. 7, A and B) had strongly overdamped response dynamics. $H_T(s)$ in these cells could be reduced to a first-order lag element, $H_T(s) = 1/(1 + s\tau_T)$, with little or no increase in fitting errors, indicating that their response dynamics in the frequency range from 0.5 to 125 Hz were dominated by a single real pole. The mean response dynamics of Type C and Type E cells (Fig. 7, C and D), on the other hand, were best fit by second-order lag elements. The gain and phase errors of Type C cells (with those for Type E cells in parentheses) for a second-order lag element were 6.2% (9.6%) and 4.4° (3.0°), respectively. The best-fitting one-term operator, $H_T(s) = 1/(1 + s\tau_T)$, with $\tau_T = 9.1$ s (13.8 s), increased these errors to 9.0% (10.8%) for gain and 7.1° (17.7°) for phase.

Differences in the low-frequency response dynamics of utricular hair cells to hair bundle displacement were largely accounted for by variations in a single parameter, k_A . Type B and Type F cells, at least for frequencies >0.5 Hz, did not exhibit adaptation and had near-zero k_A values. Type C cells, on the other hand, uniformly adapted to hair bundle displacement and had a mean k_A value of 0.24. Individual Type C cells that differed in their degree of adaptation to hair bundle displacement also differed in their values of k_A .

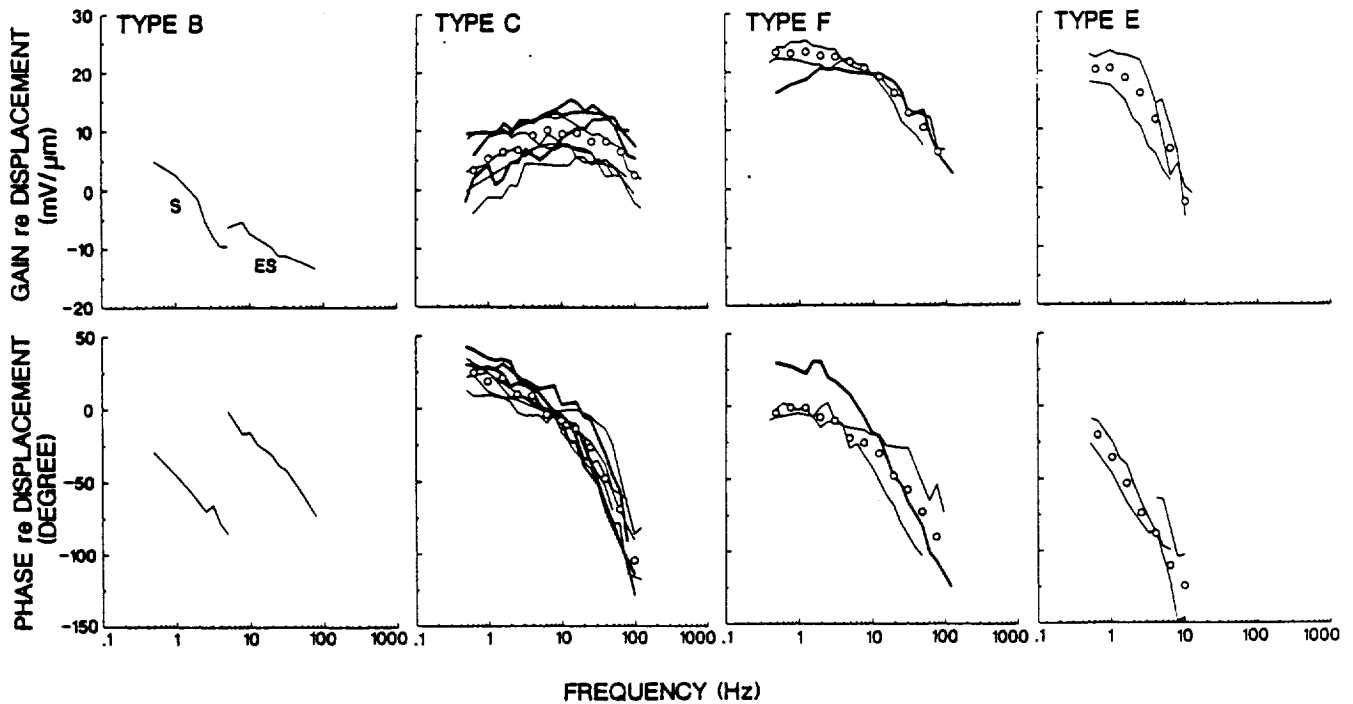


FIG. 6. Bode plots of gains (*top*) and phases (*bottom*) for 2 Type B, 8 Type C, 3 Type F, and 3 Type E cells to sinusoidal hair bundle displacement. Lines: curves for individual cells. Circles: means for all cells in each category. For Type C cells, heavy lines delineate individual curves of rapidly adapting Type C cells. For Type F cells, heavy line delineates a transitional Type F cell whose voltage response, unlike those of typical Type F cells, demonstrated adaptation to hair bundle displacement (see text). Phase leads are plotted as positive (upward) values.

with rapidly adapting Type C cells ($n = 3$) having k_A values ranging from 0.27 to 0.38 and slowly adapting Type C ($n = 5$) cells having k_A values ranging from 0.11 to 0.20. Type E

cells had intermediate k_A values, indicating that they, like Type C cells, were slowly adapting to hair bundle displacement (see below). Estimates of τ_A were only reliable when

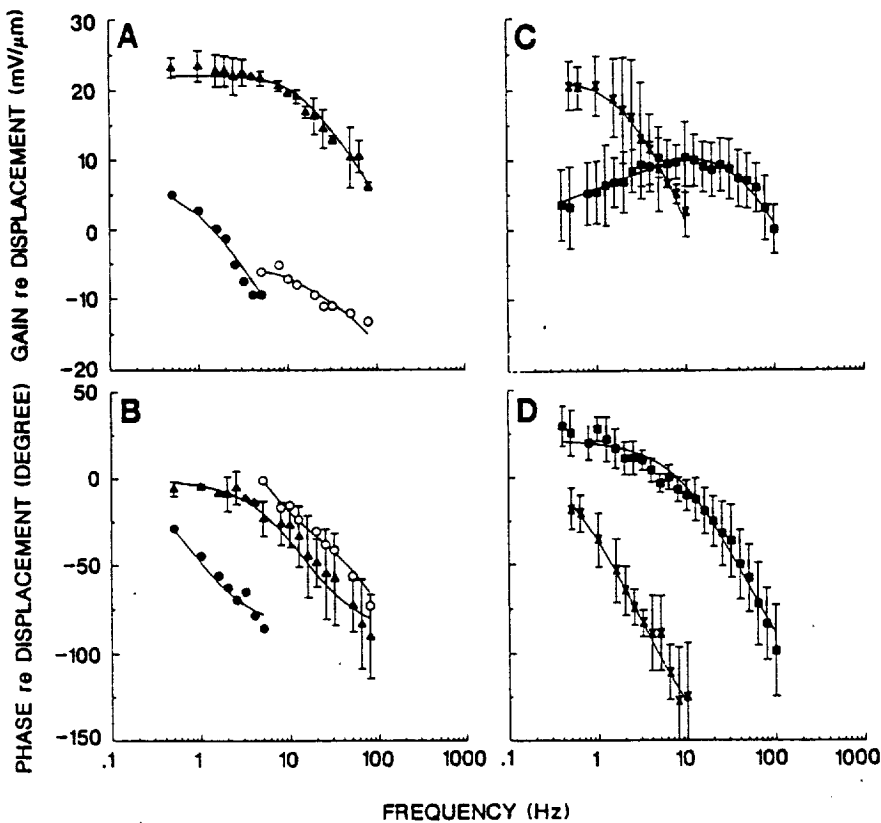


FIG. 7. Mean Bode plots of gains (*A* and *C*) and phases (*B* and *D*) for 16 hair cells in Fig. 6 to sinusoidal hair bundle displacement. Open and solid symbols: extrastriolar and striolar cells, respectively. Lines indicate best-fitting transfer functions to mean frequency response data (see text). Circles: Type B. Squares: Type C. Triangles: Type F. Crosses: Type E. Points: means. Bars: SDs.

TABLE 3. Mean transfer function parameters, hair bundle displacement

Cell Type	n	Hair Bundle Displacement			
		k_A	τ_A , s	τ_{T1} , ms	τ_{T2} , ms
Type B					
MES	1	0.00	—	5.25	0.01
MS/LS	1	0.04	—	3.00	205.0
LES	—	—	—	—	—
Type C	8	0.24	0.17	1.07	6.96
RA	3	0.35	0.12	2.35	5.61
SA	5	0.13	0.22	0.34	4.33
Type F	2	0.01	—	7.84	1982.
Type E	3	0.14	1.33	25.22	135.6

Values are means. n is number of hair cells. k_A and τ_A are the exponent and time constant of a fractional-lead operator; τ_{T1} and τ_{T2} are time constants of a 2nd-order lag operator. Three transitional cells—1 Type B, 1 Type C, and 1 Type F—are not included in the above averages (see text). RA, rapidly adapting; SA, slowly adapting. For other abbreviations, see Table 1.

the fractional-lead operator was effective (i.e., when k_A was nonzero) because large changes in τ_A could be compensated by small changes in k_A . This was true only for Type C and, to a lesser extent, Type E cells. For these cell types, estimates of τ_A were 0.17 s and 1.33 s, respectively.

Response dynamics to intracellular current and hair bundle displacement

In a previous study (Baird 1994) I examined the response dynamics of a separate population of hair cells to intracellular current. The gains of hair cells to intracellular current were constant at low frequencies and decreased with increasing frequency. These gains differed markedly, reflecting the different resistances of hair cells at resting membrane potential. The phases of hair cells in response to intracellular current hovered near zero at low frequencies and became increasingly phase lagged for increasing frequency. When possible, I examined the responses of individual hair cells to both sinusoidal intracellular current and hair bundle displacement at multiple frequencies. This was accomplished in seven cells, including six Type C cells and a Type F cell whose voltage responses closely resembled those of Type C cells. For other hair cell types this information was either unavailable or was obtained at different resting membrane potentials, preventing a direct comparison of the response dynamics to the two stimuli.

The response dynamics of hair cells to sinusoidal hair bundle displacement differed in two respects from their response dynamics to intracellular current. First, hair cells that adapted to hair bundle displacement did not adapt to intracellular current. This is seen in Fig. 8, which illustrates the Bode plots of a rapidly adapting (Fig. 8, A and B) and slowly adapting (Fig. 8, C and D) Type C cell and the mean Bode plot of six Type C cells (Fig. 8, E and F) to both intracellular current and hair bundle displacement. In each case the responses to intracellular current (open symbols) did not display the gain enhancements and large phase leads displayed by the responses to hair bundle displacement (solid symbols) at low frequencies. Rather, adapting

hair cells displayed low-pass filter characteristics in response to sinusoidal current, with constant gains and near-zero phases at low frequencies and decreasing gains and increasing phase lags at higher frequencies. Second, with the exception of one Type C cell, hair cells had higher bandwidths to hair bundle displacement than they did to intracellular current, presumably reflecting the increased conductance resulting from the opening of increased numbers of transduction channels during hair bundle displacement. This was also reflected in the time constants of the best-fitting transfer functions to individual hair cells, which were larger in response to intracellular current than to hair bundle displacement. The mean dominant time constant of six Type C cells, for example, was 2.6 s to intracellular current but only 2.2 s to hair bundle displacement.

I was unable to obtain the responses of individual Type B and Type E cells to both intracellular current and hair bundle displacement at multiple stimulus frequencies. I was, however, able to compare the responses of these cells to 5.0-Hz sinusoids of intracellular current and hair bundle displacement. In each case, hair cells displayed smaller phase lags at this frequency to hair bundle displacement than they did to intracellular current, suggesting that they had higher bandwidths to the former stimulus.

Responses to step hair bundle displacements

Because of a lack of data at low frequencies it was not always possible to determine whether hair cells were adapting using sinusoidal displacements. The low-frequency responses of hair cells to hair bundle displacement were therefore further assessed with step displacements. In general, adapting hair cells displayed adaptation to excitatory displacements that depolarized their membrane potentials. Inhibitory displacements, which hyperpolarized membrane potential, caused little or no adaptation during the step stimulus but did produce a depolarizing overshoot and subsequent adaptation at the termination of the step stimulus.

Hair cells with differing hair bundle morphology had markedly different responses to hair bundle displacement. This is illustrated in Fig. 9, which depicts typical voltage responses of each hair cell type to both excitatory hair bundle displacement (*left*) and, if available, intracellular current (*right*). Type B cells in both the striolar ($n = 1$) and extrastriolar ($n = 1$) regions displayed little or no adaptation to maintained hair bundle displacement. The responses of these cells to step displacement strongly resembled their responses to steps of intracellular current. Hair cells restricted to the striolar region, on the other hand, had different responses to hair bundle displacement and intracellular current, displaying a marked adaptation to the former but not the latter stimulus. This adaptation took the form of response declines during step displacements and hyperpolarizing undershoots at their termination. The rate and extent of adaptation differed in different hair cells. As for sinusoidal stimuli, Type C cells had either rapidly or slowly adapting responses. Rapidly adapting Type C cells ($n = 4$), after initially rising to a peak value, declined in <50–100 ms to a small steady-state level. Other Type C cells ($n = 3$) had slower rates of adaptation, declining within 100–200 ms to larger steady-state levels. The rate of

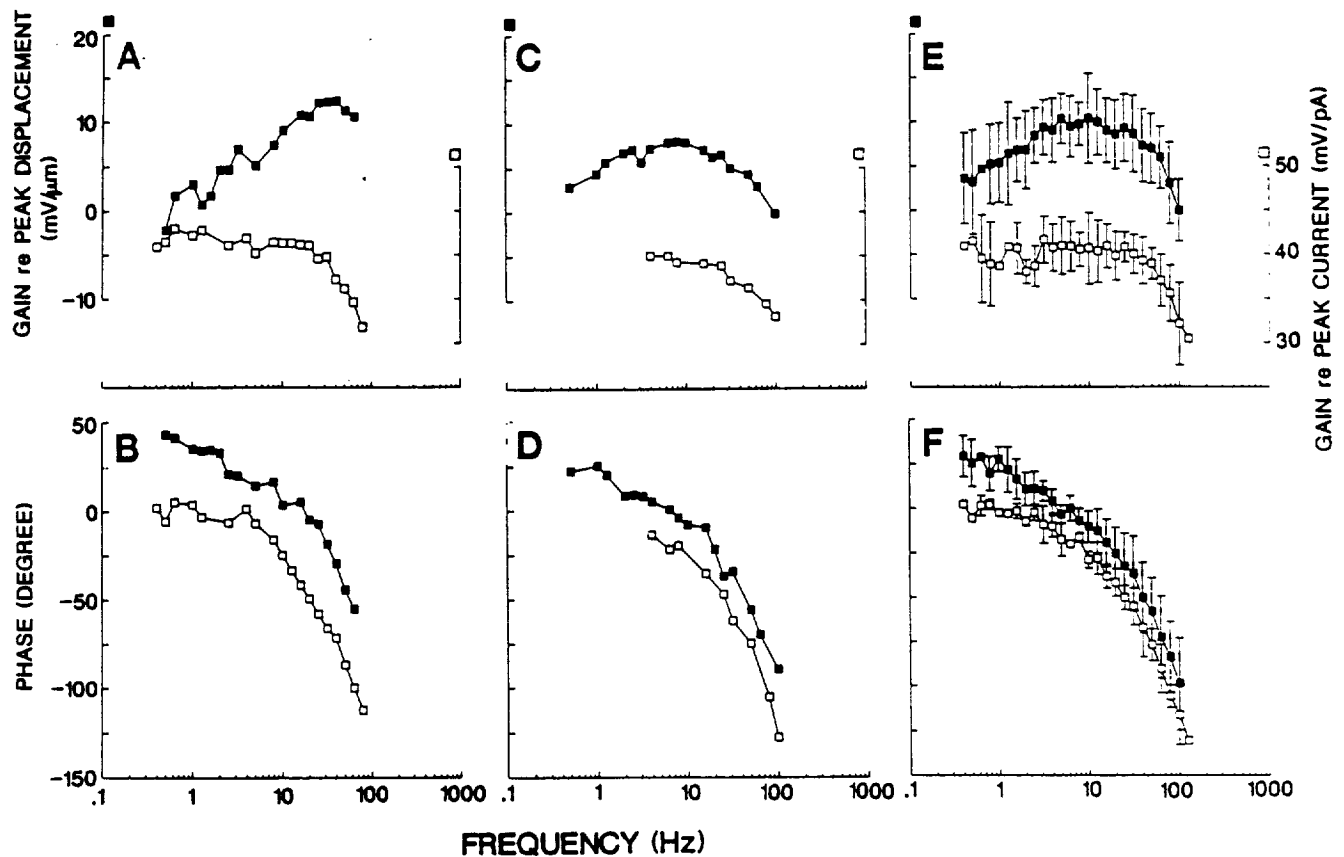


FIG. 8. Bode plots of gains and phases of individual rapidly (*A* and *B*) and slowly (*C* and *D*) adapting Type C cells and mean Bode plots of 6 Type C cells (*E* and *F*) to sinusoidal intracellular current (open squares) and hair bundle displacement (solid squares). Points: means. Bars: SDs.

adaptation of Type C cells to step displacement, as for sinusoidal stimuli, was correlated with their macular location, with rapidly and slowly adapting cells located in the outer and inner striolar rows, respectively. Type F ($n = 4$) and Type E ($n = 2$) cells adapted very slowly, reaching steady-state values in 300–500 ms, and displayed pronounced hyperpolarizing undershoots at the termination of excitatory step displacements. In Type E cells these hyperpolarizing undershoots were also seen, albeit to a smaller extent, in the responses to intracellular current. With the exception of Type E cells, rapidly adapting cells declined to a greater extent than slowly adapting cells. Type E cells, although slowly adapting, displayed large response declines to step displacement.

There was good agreement between the time constants of adaptation measured in the time and frequency domain. In four rapidly adapting Type C cells the mean time constant of adaptation to step displacement, measured as the time constant of the best-fitting exponential, was equal to 0.06 s, a value in reasonable agreement with 0.12 s, the time constant obtained from the best-fitting transfer function for three rapidly adapting Type C cells to sinusoidal stimulation (Table 3). A similar result was obtained for slowly adapting Type C cells, for which the time constants of adaptation to step and sinusoidal displacement were 0.20 s and 0.22 s, respectively. The best-fitting transfer functions for each hair cell type, summarized in Table 3, were also used to derive theoretical responses of these hair cells to step

displacement (data not shown). Parameters used in these calculations were, with the exception of a constant gain term, derived from the mean Bode plots of each hair cell type. With one exception, the predicted response declines after excitatory step displacements were close to that actually observed. The one discrepancy involved the time course of the hyperpolarizing undershoot after the response decline in rapidly adapting Type C cells, which was more pronounced than that seen in response to step displacements.

Adaptation versus step amplitude

The peak and steady-state responses of hair cells were examined to excitatory step displacements of varying amplitude (Fig. 10). For small amplitudes the peak responses of hair cells to hair bundle displacement were linearly related to the amplitude of hair bundle displacement. At larger amplitudes the peak responses of hair cells began to saturate. The range of linear response and sensitivity to hair bundle displacement was different in different hair cell types. Type B cells, for example, produced the smallest voltage responses to hair bundle displacement. These responses, however, were linear over a wide range, barely displaying saturation at 2- μm displacements. Type C cells produced larger voltage responses but only over a narrower range, displaying saturation for hair bundle displacements $>1 \mu\text{m}$. Type F and Type E cells had the large voltage re-

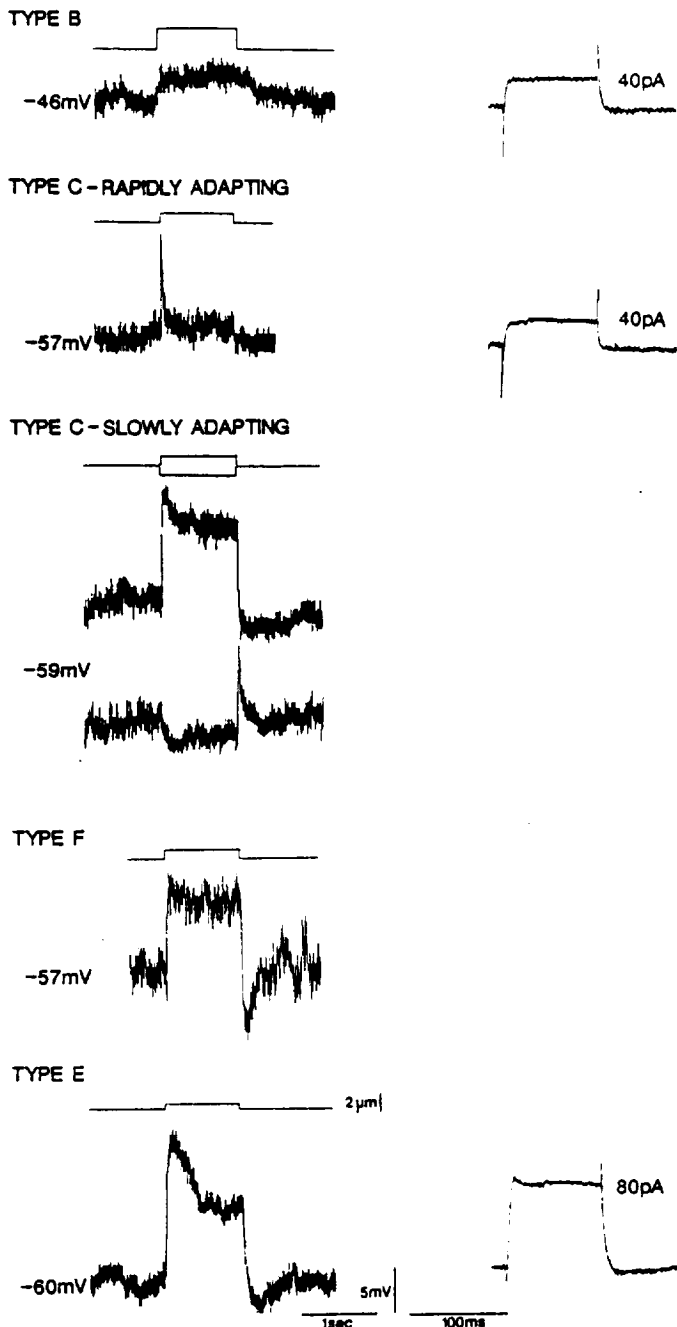


FIG. 9. Voltage responses of typical Type B, Type C, Type F, and Type E cells to steps of hair bundle displacement (*left*) and intracellular current (*right*). Numbers at *left* and *right* indicate the resting membrane potential of the cell and the amplitude of the current stimulus, respectively.

sponses but most restricted linear range of all utricular hair cells, displaying saturation for step displacements $>0.5 \mu\text{m}$. With the exception of Type B cells, the lengths of the longest stereocilia of striolar hair cells were similar (Table 1), indicating that this discrepancy was not due merely to the way in which hair cells were stimulated in this study. The time course of adaptation, at least for displacements in the linear operating range, was not a function of stimulus amplitude.

With the possible exception of rapidly adapting Type C cells, the steady-state responses of adapting hair cells, at

least for small step amplitudes, were also linearly related to step amplitude. The steady-state responses of rapidly adapting Type C cells were relatively independent of stimulus amplitude, although this was difficult to measure because of the small size of these responses. Thus the extent of adaptation, as measured by the inverse ratio of the peak and steady-state responses, was independent of stimulus amplitude. The extent of adaptation was also, as mentioned above, different in different hair cell types, being least in Type F cells and greatest in rapidly adapting Type C cells.

The steady-state sensitivities of Type B hair cells, whether in the striolar or extrastriolar region, to step stimulation were in reasonable agreement with their sensitivities to low-frequency sinusoidal stimulation (Table 4), suggesting that these cells do not adapt to maintained hair bundle displacement. The sensitivity of a Type B cell in the medial extrastriola to step displacement and 5.0-Hz sinusoidal displacement, for example, was 0.63 and 0.59 $\text{mV}/\mu\text{m}$. For a striolar Type B cell the sensitivity to step displacement and 0.5-Hz sinusoids was 1.95 and 1.18 $\text{mV}/\mu\text{m}$, respectively. The mean sensitivity of Type F cells to step displacement, on the other hand, was significantly less than their sensitivity to 0.5 Hz sinusoidal stimulation (8.58 and 13.23 $\text{mV}/\mu\text{m}$, respectively). This suggests that although little evidence of adaptation was seen in these cells in response to sinusoidal stimulation (Figs. 5-7), Type F cells do adapt to very low-frequency displacement. This suggestion is further supported by the results of studies using long-duration step displacements (see below). As expected, the sensitivities of Type C and Type E cells to step displacement were also less than their sensitivities to low-frequency sinusoidal stimulation, confirming that they also adapt to maintained hair bundle displacement. Type C cells, for example, had mean sensitivities of 1.11 $\text{mV}/\mu\text{m}$ to step displacement and 1.56 $\text{mV}/\mu\text{m}$ to 0.5-Hz sinusoidal displacement. The mean sensitivities of Type E cells to the same stimuli were 9.68 and 11.12, respectively.

Adaptation versus step duration

The effects of increasing step duration on adaptation were examined at step durations ranging from 100 ms to 10 s (Fig. 11). In nonadapting Type B cells there was no sign of adaptation to either 1- or 2-s step displacements. Other hair cell types, however, displayed increasing amounts of adaptation at longer maintained hair bundle displacements. This was seen most clearly in Type F cells, which were relatively nonadapting at 100- and 200-ms step displacements but demonstrated increasing amounts of adaptation in response to steps of longer duration. In rapidly adapting Type C cells (data not shown) the time course of adaptation was similar at all step durations, confirming that adaptation in these cells is completed before 100 ms. I did not record the responses of these hair cells to shorter step durations. More slowly adapting Type C hair cells, on the other hand, had different time courses for different step durations. In slowly adapting Type E cells adaptation continued despite a lack of maintained stimulus, suggesting that adaptation was activated by the excitatory hair bundle displacement but delayed by the kinetics of some intermediate process. This delay may reflect the kinetics of calcium regulation in dif-

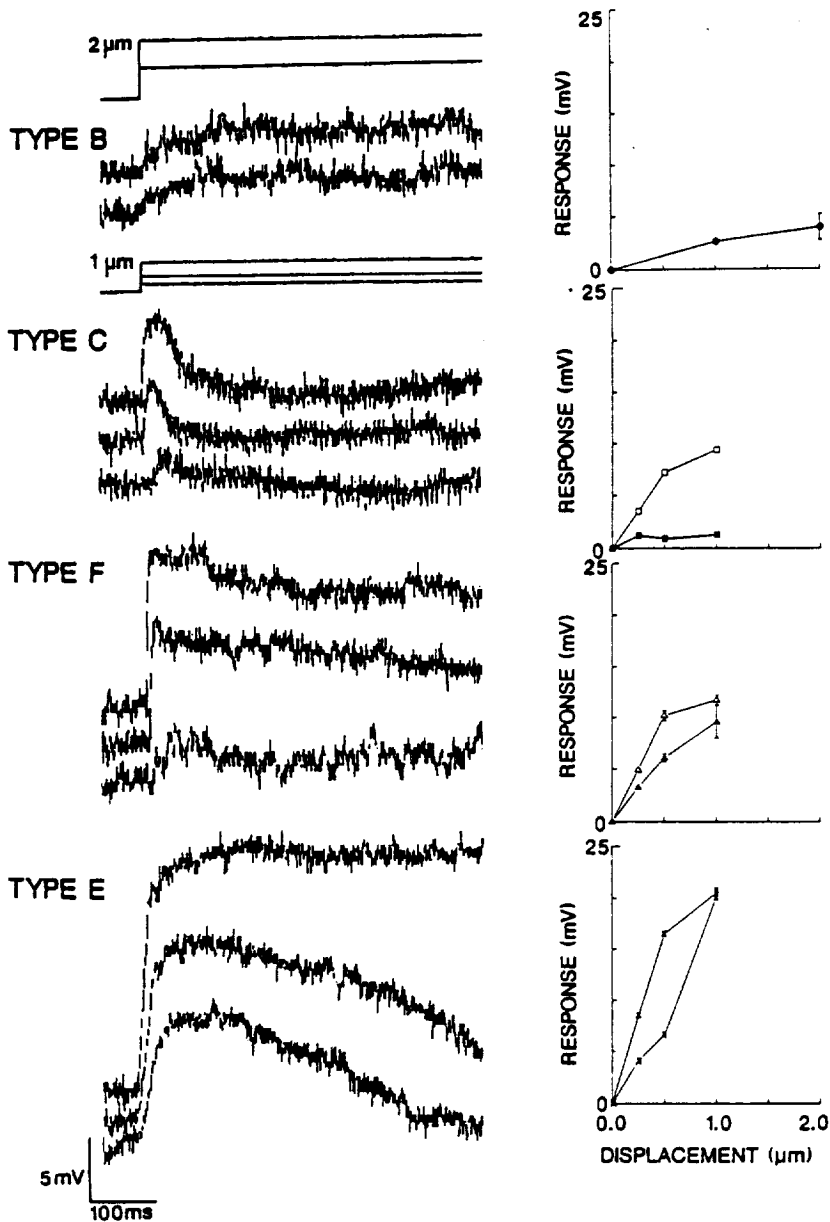


FIG. 10. Voltage responses of typical Type B, Type C, Type F, and Type E hair cells to step hair bundle displacements of varying amplitude. Peak (open symbols) and steady-state (solid symbols) responses for each hair cell are plotted vs. hair bundle displacement to the right. Circles: Type B. Squares: Type C. Triangles: Type F. Crosses: Type E. Points: means. Bars: SDs.

ferent hair cell types and may be the rate-limiting step in determining the kinetics of the adaptation process in different hair cell types (see below).

DISCUSSION

In the companion paper (Baird 1994) I demonstrated that utricular hair cells in different macular zones differed in their responses to intracellular current, implying that these cells differed in their complement of basolateral membrane conductances. In this study I demonstrate that utricular hair cells in different macular zones also differ in their sensitivity and response dynamics to hair bundle displacement. Because the response dynamics of hair cells to intracellular current differ from those to hair bundle displacement I argue that these differences arise not from the passive or active membrane properties of hair cells but rather from an adaptation process associated with mechano-electric transduction. Adaptation, by preventing tonic dis-

placements from saturating the mechano-electric response, allows hair cells to maintain sensitivity to higher-frequency displacements. More specifically I suggest that utricular hair cells vary in their rate of adaptation to maintained hair bundle displacement, regulating their sensitivity and frequency selectivity and allowing some hair cell types to encode static gravity and others to encode high-frequency linear acceleration.

Previous studies have demonstrated that adaptation is not a universal property of hair cells. Hair cells in chick vestibular endorgans (Ohmori 1985, 1987) and the mammalian cochlea (Russell et al. 1989), for example, do not adapt at all to hair bundle displacement. Hair cells in different endorgans are also known to differ in their rates of adaptation. In the turtle cochlea (Crawford et al. 1989, 1991), for example, hair cells adapt an order of magnitude faster than do hair cells in the bullfrog sacculus (Assad et al. 1989; Eatock et al. 1987; Hacohen et al. 1989). Hair cells within individual endorgans, however, tend to have similar adapta-

TABLE 4. Response gains, step and sinusoidal hair bundle displacements

Cell Type	Sinusoidal Displacements Gain		Step Displacements Gain	
	0.5 Hz, mV/ μ m	5.0 Hz, mV/ μ m	Peak, mV/ μ m	Steady-State, mV/ μ m
Type B	1.18 (1)	0.52 \pm 0.18 (6)	—	1.29 \pm 0.93 (2)
MES	—	0.59 \pm 0.25 (3)	—	0.63 (1)
MS/LS	1.18 (1)	0.46 \pm 0.08 (3)	—	1.95 (1)
LES	—	—	—	—
Type C	1.56 \pm 0.91 (8)	2.83 \pm 1.30 (12)	5.49 \pm 1.69 (7)	1.11 \pm 0.62 (7)
Type F	13.23 \pm 2.90 (3)	9.66 \pm 2.36 (7)	10.19 \pm 1.22 (4)	8.58 \pm 2.98 (4)
Type E	11.12 \pm 4.27 (2)	2.94 \pm 1.69 (4)	13.25 \pm 4.60 (2)	9.68 \pm 1.16 (2)

Values are means \pm SD with sample numbers in parentheses. Three transitional units—1 Type B, 1 Type C, and 1 Type F—are not included in the above averages (see text). For abbreviations, see Table 1.

tion kinetics. To my knowledge these results are the first direct evidence of large-scale regional differences in adaptation in hair cells from a single inner-ear endorgan.

Sensitivity of hair cells to hair bundle displacement

My results reveal that hair cells with differing hair bundle morphology have different sensitivities to hair bundle displacement. More specifically, Type B and, to a lesser extent, Type C cells have lower sensitivities to hair bundle displacement than Type F and Type E cells. This was not due to the manner in which hair bundles were stimulated in this study. It was, however, partially determined by geometric factors associated with the hair bundle morphology of different hair cell types. As long as hair bundle displacement is applied at the tip of the hair bundle, longer hair bundles are less sensitive to hair bundle displacement. They will, however, linearly transduce a wider range of displacements. In many vestibular hair cells this process is further extended by using a long kinocilium to effectively increase stereociliary length. Hair bundles with large numbers of short stereocilia are also more sensitive than other hair bundles, because small displacements produce large angular rotations and because more stereocilia imply more transducer channels. When normalized for these geometric factors, however, the sensitivities of utricular hair cell types were still markedly different, demonstrating that differences in hair bundle morphology can only partially compensate for intrinsic differences in sensitivity between hair cell types. Other factors, not examined in this analysis, may also contribute to differences in sensitivity between hair cell types. It is possible, for example, that utricular hair cells differ in the size of their transduction conductances, the range of tension conveyed by tip links to their transduction channels, or the probability of opening of their transduction channels.

Differences in the sensitivity of utricular hair cells to hair bundle displacement might also reflect differences in the passive membrane properties of distinct hair cell types (Baird 1994). The sensitivity of hair cells to hair bundle displacement, however, did not correlate with their sensitivity to intracellular current. Type B cells, for example, had high input resistances but low sensitivities to hair bundle displacement. Type C cells, by contrast, had low resistances

and large responses to hair bundle displacement. When normalized for differences in hair bundle morphology, the maximum sensitivities of utricular hair cells to hair bundle displacement were similar to those reported for other hair cell preparations. Hair cells in the turtle (Crawford et al. 1989) and mammalian cochlea (Russell et al. 1986) have maximum sensitivities of 30 mV/ $^{\circ}$. Vestibular hair cells have somewhat lower sensitivities. Hair cells in the bullfrog sacculus, for example, have reported sensitivities from 2–4 mV/ $^{\circ}$ (Eatock et al. 1987; Hudspeth and Corey 1977).

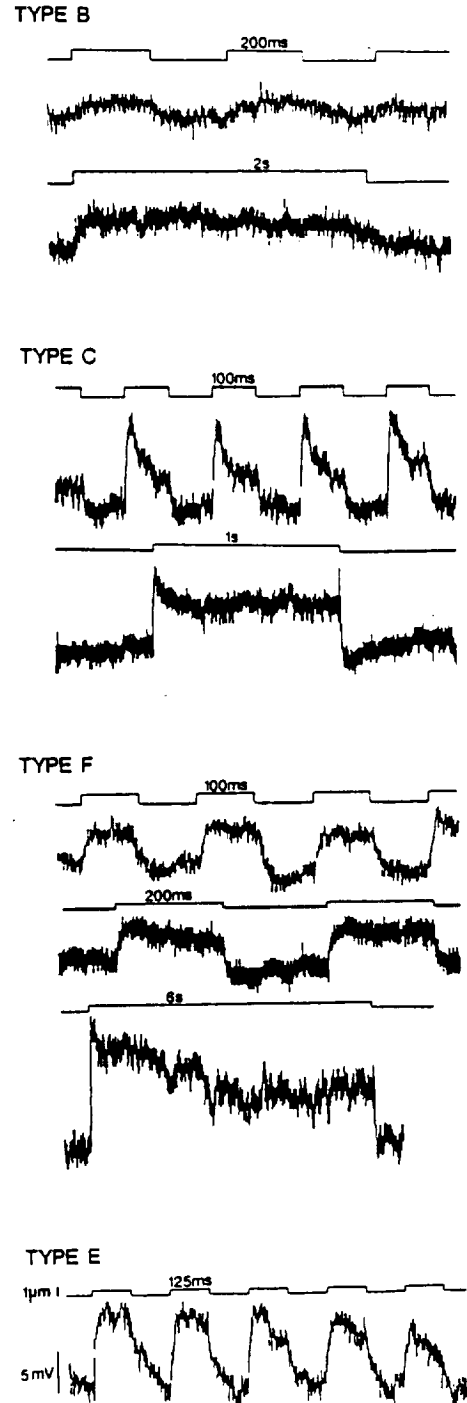


FIG. 11. Voltage responses of typical Type B, Type C, Type F, and Type E hair cells to step hair bundle displacements of varying duration.

This compares favorably with my value of $2 \text{ mV}/^\circ$ for Type F and Type E cells. Type B cells, on the other hand, had sensitivities of only $0.1 \text{ mV}/^\circ$.

Hair cells in the bullfrog utricle also differed in their linear range of transduction, suggesting that the relationship between hair bundle displacement and the probability of transduction channel opening is different in different hair cell types. Previous studies in auditory (Fuchs et al. 1988; Russell et al. 1986) and chick vestibular (Ohmori 1985, 1987) hair cells have also shown that hair cells with longer hair bundles differ in their linear range and sensitivity to hair bundle displacement. The linear range of utricular hair cells ranged from 3° in Type F and Type E cells to $\sim 25^\circ$ in Type B cells and was similar to that reported for other preparations. In the turtle cochlea, hair cells encode $<5^\circ$ of angular rotation (Crawford et al. 1989). This range is somewhat larger in vestibular hair cells, ranging from $\sim 7^\circ$ for chick vestibular hair cells (Ohmori 1984, 1985) to $\sim 15^\circ$ for hair cells in the bullfrog sacculus (Hudspeth and Corey 1977).

Response dynamics of hair cells to hair bundle displacement

The response dynamics of utricular hair cells to hair bundle displacement, measured in both the time and frequency domain, differ from those to intracellular current. More specifically many hair cells display adaptation, recognizable by conspicuous response declines to maintained step displacements and large gain enhancements and phase leads to low-frequency sinusoidal displacement. This is a function of their macular location, with striolar but not extrastriolar cells adapting to hair bundle displacement. Among adapting cells the rate and extent of adaptation differs in different hair cell types. These differences are also correlated with macular location, with rapidly adapting cells located in the outer striolar rows and more slowly adapting cells located more centrally. The step responses of Type C cells in the outer rows, for example, are rapidly adapting. Type C cells located more centrally adapt somewhat more slowly to maintained displacement. Type F and Type E cells, located only in the inner striolar rows, adapt only in response to longer-duration step displacements. With the exception of Type E cells, the rate and extent of hair cells are also correlated, with rapidly adapting cells adapting to a greater extent than more slowly adapting hair cells.

Similar response declines to step displacements are seen in intracellular recordings of receptor voltage from hair cells in the bullfrog sacculus (Eatock et al. 1987). In this preparation the responses of hair cells decline to 10–30% of their peak amplitude in response to depolarizing step displacements. Adaptation also manifests itself as a decline in the receptor current of voltage-clamped hair cells in both the bullfrog sacculus (Assad et al. 1989; Eatock et al. 1987; Hacohen et al. 1989) and turtle cochlea (Crawford et al. 1989, 1991) to maintained hair bundle displacement. The extent of adaptation is similar in auditory and vibratory hair cells. Its time course, however, is not. The responses of hair cells in the bullfrog sacculus decline to steady-state levels in $<50 \text{ ms}$ in response to depolarizing step displacements. Hair cells in the turtle cochlea adapt even more

quickly, declining within 10 ms to $\sim 20\%$ of their peak amplitude (Crawford et al. 1989). No evidence for adaptation has been seen in hair cells from the chick vestibular endorgans (Ohmori 1985, 1987) or the mammalian cochlea (Russell et al. 1989).

Adaptation in other inner ear endorgans, although it manifests itself as a progressive decline in receptor current or voltage, is not due to desensitization of the transducer channels (Assad et al. 1989; Crawford et al. 1989; Eatock et al. 1987; Hacohen et al. 1989). Rather, transduction persists with normal sensitivity, but the position at which the hair cell is most sensitive shifts from its initial resting position toward the current position of the hair bundle. Thus adaptation involves a mechanical adjustment of the tension stimulus reaching the displacement-sensitive stereocilia (Assad et al. 1989; Hacohen et al. 1989; Howard and Hudspeth 1987, 1988) or an adjustment of the open probabilities of the transduction channel (Crawford et al. 1989, 1991). This adjustment is believed to be made at the level of the tip links, fine filamentous links connecting adjacent stereocilia within the hair bundle (Osborne et al. 1988; Pickles et al. 1984). Mechanoelectric transduction is disrupted when these links are severed by removal of calcium from the external medium (Assad et al. 1991; Crawford et al. 1991). Recent physiological evidence suggests that a cytoplasmic motor, possibly a myosinlike protein (Hacohen et al. 1989; Howard and Hudspeth 1987, 1988; Shepherd et al. 1990), maintains resting tension on transduction channels, perhaps by actively moving one or both ends of the tip links.

Before concluding that response declines seen in utricular hair cells are the result of an adaptation process associated with mechanoelectric transduction I must briefly consider some potential artifacts and alternative explanations for their generation. The observed declines in these voltage responses are unlikely to be an artifact due to the slipping of the stimulus probe. First, there was no observable motion of the top of the hair bundle and stimulus probes did not appear to lose contact with the hair bundle during an adapting stimulus. Second, the steady-state voltage responses of adapting hair cells did not exhibit further changes after adaptation had taken place, even for step displacements $\leq 10 \text{ s}$ in duration, suggesting that the probe was well coupled to the hair bundle. Finally, the time course of adaptation was different in different hair cell types. Because the hair bundles of all hair cells were displaced in a similar manner, it seems unlikely that slippage of the stimulus probe would occur only for specific hair cell types.

Unlike other studies in the bullfrog sacculus (Assad et al. 1989; Hacohen et al. 1989) and turtle cochlea (Crawford et al. 1989, 1991), I did not directly record transduction current in these experiments. It is therefore possible that at least some of the response dynamics seen in response to hair bundle displacement were contributed by the gating kinetics of voltage- and ion-dependent conductances in the basolateral membrane. Differences in the response dynamics of utricular hair cells to hair bundle displacement would then reflect differences in the active membrane properties of distinct hair cell types (Baird 1994). Several lines of evidence, however, suggest that this is unlikely. The amplitude of voltage responses examined in this study was small. With the possible exception of Type C cells, which

may possess a persistent membrane conductance near resting membrane potential (Baird 1994), it is therefore unlikely that voltage-dependent membrane conductances were activated to any large extent in response to the range of hair bundle displacements used in this study. Moreover, the low-frequency response dynamics of hair cells to hair bundle displacement were markedly different from those to intracellular current. Individual hair cells that adapted to hair bundle displacement, for example, did not adapt to intracellular current. In addition, hair cells that had similar response dynamics to intracellular current had very different response dynamics to hair bundle displacement. I cannot as yet rule out the possibility that the response declines seen in the responses of utricular hair cells are due to an inactivation of their transduction channels. The most parsimonious interpretation of these results, however, is that, as in the bullfrog sacculus (Assad et al. 1989; Eatock et al. 1987; Hacohen et al. 1989) and turtle cochlea (Crawford et al. 1989, 1991), adaptation acts to reduce the mechanical input to the transducer channels, resetting the operating range of the hair bundle.

It is important to establish that differences in adaptation kinetics are not an artifact determined by variations in the physiological state of hair cells during recording. Adaptation in hair cells is known to be more labile than mechanoelectric transduction (Assad et al. 1989; Eatock et al. 1987) and has even been compromised in early whole-cell patch-clamp recordings (Holton and Hudspeth 1986). This is probably due to the known tendency for patch-clamp electrodes to dialyze cells, leaching the intracellular cytoplasm of important cofactors or second messengers necessary for many physiological phenomenon (Marty and Neher 1983). The sharp intracellular microelectrodes used in this study would not be expected to produce such an effect. Moreover, if such a mechanism were at work, one might expect to see adapting cells only at early times during an experiment or to find substantial disagreement between intracellular data acquired at different times from the same hair cell. Neither of these possibilities was observed.

There are still several potential difficulties with concluding that adaptation kinetics vary in different hair cell types. First, the number of hair cells recorded in this study was small and these cells were located only within the striola or immediately adjacent to its medial border. A larger and more widely dispersed sample of hair cells, particularly in the extrastriolar regions, would be desirable. Because of the limited data set, many of my interpretations about the rate and extent of adaptation in different hair cell types should be viewed cautiously. In addition, hair cells were not always stimulated at identical resting membrane potentials. In other preparations (Assad et al. 1989; Crawford et al. 1989; Hacohen et al. 1989), depolarizing membrane voltages have been shown to shift the resting DRCs of hair cells to the left, decreasing both the size of the response and the rate of adaptation to a given hair bundle displacement. I would therefore expect adaptation to be more difficult to detect in hair cells with more depolarized resting membrane potentials. Furthermore, the rate of any observed adaptation would be underestimated in these cells. It is therefore possible that nonadapting hair cells were simply recorded at more depolarized resting membrane potentials than rapidly

adapting cells. This was not observed. Rather, rapidly adapting hair cells often had more depolarized resting membrane potentials than more slowly adapting hair cells. Furthermore, hair cells with similar resting membrane potentials often displayed markedly different rates of adaptation to hair bundle displacement.

A second possibility is that some hair cells were driven into negative or positive saturation by the placement of the stimulating probe, obscuring the presence of adaptation to maintained hair bundle displacement. To guard against this possibility, I was careful to compare the resting membrane potential of hair cells before and after placement of the stimulating probe and to examine the form of the DRC. It is nevertheless possible that the hair bundles of some hair cells were displaced from their resting position by the stimulus probe, especially with the relatively large displacements used in these experiments. This is supported by the observation that nonadapting hair cells were extremely sensitive to resting hair bundle position and were easily driven into negative or positive saturation. Rapidly adapting hair cells, however, were not sensitive to resting hair bundle position, suggesting that utricular hair cells do differ in their adaptation kinetics.

A third potential difficulty with these studies was that hair cells were not always stimulated at identical displacements. The process underlying adaptation in auditory and vibratory hair cells is nonlinear, occurring more rapidly for excitatory than for inhibitory steps and more completely for small than for large steps (Assad et al. 1989; Crawford et al. 1989, 1991; Eatock et al. 1987; Hacohen et al. 1989). In these preparations, the time course of the response to adapting steps of varying amplitude follows roughly similar time courses, so long as hair bundle displacement is kept below a certain level. At saturating hair bundle displacements, however, the time course of the voltage response does not reflect the actual time course of adaptation. It is therefore possible that I underestimated the rate of adaptation in some hair cells. Voltage responses in Type B cells, for example, were small and, unlike other hair cell types, observed only for large hair bundle displacements. It is possible that these cells would have exhibited faster rates of adaptation at smaller stimulus amplitudes. Hair cells stimulated with similar displacements, however, still differed dramatically in their rate of adaptation to hair bundle displacement, supporting the conclusion that large variations exist in the adaptation kinetics of utricular hair cells.

Differences in the response dynamics of utricular hair cells to hair bundle displacement were correlated with differences in hair bundle morphology rather than macular location per se. Type B cells, for example, had similar response properties, whether they were located in the striolar or extrastriolar region. Moreover, hair cells in similar macular locations, but with differing hair bundle morphology, differed in their responses to hair bundle displacement. Type C cells in the inner striolar rows, for example, were more rapidly adapting than other cell types in these rows. At the same time, the relation between adaptation kinetics and hair bundle morphology was not absolute. The adaptation kinetics of Type C cells, for example, varied over a wide range. A few hair cells also had intermediate physiological properties. Hair cells on the striolar border, for exam-

ple, could be nonadapting, resembling Type B cells, or rapidly adapting, resembling the responses of Type C cells. This was also seen in the striolar region, where the responses of one Type F cell strongly resembled those of Type C cells. These transitional units may have been inadvertently misclassified. The fact that these cells were all located in transitional macular locations, however, suggests that they may represent natural variations.

Previous studies in both the bullfrog sacculus (Assad et al. 1989; Hacohen et al. 1989) and the turtle cochlea (Crawford et al. 1989, 1991) have shown that the kinetics of adaptation are a function of both membrane voltage and calcium concentration. As Assad et al. (1989) and Crawford et al. (1989) have shown, both the decline in receptor current and the shift in the DRC of adapting hair cells are slower at depolarized potentials. This voltage dependence is eliminated if extracellular calcium concentration is reduced (Assad et al. 1989), suggesting that this dependence is an indirect consequence of external calcium entry through transduction channels and that the entry of external calcium into the stereocilia facilitates the adaptation process. The rate of adaptation is also reduced by lowering extracellular calcium concentration (Eatock et al. 1987; Hacohen et al. 1989) or by including high concentrations of the calcium chelator bis-(*O*-aminophenoxy)-*N,N,N',N'*-tetraacetic acid in the interior of patch-clamp pipettes (Crawford et al. 1989). Calcium may also directly affect the kinetics of the transduction channel (Crawford et al. 1989, 1991). In either case, it appears likely that adaptation is predicated on the action of calcium at some internal site and may be slowed or prevented by limiting the access of calcium to this site. Thus the dynamics of calcium regulation within the hair bundle, which are interposed between tip-link displacement and the relaxation of tension to the transduction channels, may constitute a rate-limiting intermediate process that controls adaptation kinetics.

Calcium regulation within the hair bundle is unlikely to be accomplished entirely by passive diffusion. As Crawford et al. (1989) point out, the kinetics of adaptation are nonlinear, with the rate of adaptation being slower for larger transduction currents. This is the opposite of what would be expected from the entry of external calcium followed by passive diffusion. More likely, calcium is actively sequestered by Ca^{2+} -binding proteins that act to limit free calcium concentration within the hair bundle. The dynamics of calcium regulation would then be governed by the relative affinities of individual Ca^{2+} -binding proteins for calcium. The role of Ca^{2+} -binding proteins in regulating adaptation is not clear, although the rate of adaptation is reduced by nonselective calmodulin inhibitors (Corey et al. 1987).

Utricular hair cells with differing rates of adaptation may possess different complements of Ca^{2+} -binding proteins. Some support for this suggestion is found in the results of recent biochemical (Gillespie and Hudspeth 1991; Shepherd et al. 1989), immunocytochemical (Dechesne and Thomasset 1988; Dechesne et al. 1988; Oberholtzer et al. 1988; Rabie et al. 1983; Sans et al. 1986, 1987; Shepherd et al. 1989), and molecular biological (Dememes et al. 1991) studies. These studies have demonstrated the presence of

several Ca^{2+} -binding proteins, including calbindin (Dechesne and Thomasset 1988; Dechesne et al. 1988; Oberholtzer et al. 1988; Rabie et al. 1983; Sans et al. 1986, 1987), calmodulin (Shepherd et al. 1989), calretinin (Dechesne et al. 1991), and S-100 (Saidel et al. 1990) in auditory and vestibular hair cells. In bullfrog saccular hair cells these proteins have been localized to the hair bundle, suggesting that they are involved with mechanoelectric transduction (Gillespie and Hudspeth 1991; Shepherd et al. 1989). In addition, recent studies in our laboratory (Baird and Schuff, unpublished data) have demonstrated that utricular hair cells differ in their complement of Ca^{2+} -binding proteins.

Functional organization of the utricular macula

Hair cells in the bullfrog utricle are specialized, via a combination of mechanical and ionic mechanisms, to encode both static and dynamic acceleration. Sensitivity, for example, is determined both by mechanical factors associated with hair bundles and by the passive membrane properties of hair cells. Response dynamics, on the other hand, are governed by the kinetics of an adaptation process associated with transduction channels and of voltage-dependent conductances in the basolateral membrane. Thus Type B cells, with their long kinocilium and short stereocilia, have lower sensitivities to stereociliary displacement than other utricular hair cells. This lower sensitivity, although somewhat offset by the higher sensitivity of these cells to intracellular current (Baird 1994), allows them to faithfully transduce a wider range of hair bundle displacements than other hair cell types. Type B cells also do not adapt or adapt only very slowly to maintained hair bundle displacement. They are therefore well suited for encoding static gravity and low-frequency linear acceleration. Hair cells restricted to the striolar region, on the other hand, have higher sensitivities to natural stimulation. Moreover, they have higher frequency sensitivities than extrastriolar hair cells, and, in the case of Type E cells, are electrically tuned to further enhance their high-frequency sensitivity (Baird 1994). Type C cells, for example, resemble Type B cells in having relatively low sensitivities to hair bundle displacement. Unlike Type B cells, however, they rapidly adapt to maintained hair bundle displacement. The rapid adaptation of Type C cells has two consequences. First, it prevents static gravity from saturating their responses, allowing them to maintain high sensitivity to smaller, high-frequency linear accelerations. Second, it reduces their input conductance at the termination of depolarizing displacements, allowing them to respond to signals over a wider dynamic range (Crawford et al. 1989). In the inner striola, Type F and Type E cells have higher sensitivities and transduce a smaller range of displacement than other hair cells. They also adapt, although more slowly, to maintained hair bundle displacement. The slower time course of adaptation in these cells may enable them to retain a higher degree of sensitivity to low-frequency displacement. This would presumably reduce the sensitivity of these cells to high-frequency displacement but might allow them to retain sensitivity to both static and dynamic acceleration.

Contribution of hair cell adaptation to afferent response dynamics

Utricular afferents in bullfrog (Baird and Lewis 1986; Blanks and Precht 1976; Caston et al. 1977) and fish (Macadar et al. 1975) have previously been classified as gravity or vibratory sensitive. Gravity afferents have been further classified into three classes according to their responses to head tilt. Tonic gravity afferents respond to head position, phasic gravity afferents respond to head velocity, and phasic-tonic afferents respond to both head position and velocity. Higher vertebrates possess only tonic and phasic-tonic otolith afferents (Anderson et al. 1978; Fernandez and Goldberg 1976a,b; Goldberg et al. 1990a; Perachio and Correia 1983; Vidal et al. 1971).

Morphophysiological studies suggest that differences in afferent response dynamics are solely determined by regional variations in presynaptic transduction mechanisms (Baird et al. 1988; Goldberg et al. 1985, 1990b). In the semicircular canal, regional variations in cupular dynamics (Boyle et al. 1991; Hillman and McLaren 1979; Honrubia et al. 1981, 1989; McLaren and Hillman 1979) or the coupling of the cupula to the sensory hair bundles of hair cells (Honrubia et al. 1981, 1989; Lim 1976) may underlie the diversity in response dynamics. In the otolith organs, on the other hand, differences in afferent response dynamics may be determined by differences in the transduction mechanisms of different hair cell types. In the bullfrog utricle, the response dynamics of utricular afferents are correlated with the hair bundle morphology of their innervated hair cells (Baird and Lewis 1986), suggesting that hair cells with differing hair bundle morphology may represent independent hair cell types with distinctive physiological response properties.

These results suggest that the response dynamics of gravity afferents are largely determined by the rate of adaptation in their innervated hair cells. Tonic gravity afferents, for example, innervate Type B cells in the medial and lateral extrastriolar regions (Baird and Lewis 1986). Other afferent classes supply the striolar region, generally innervating a complex mixture of hair cell types (Baird and Schuff 1994). Phasic and phasic-tonic gravity afferents, for example, are both known to innervate hair cells in the outer striolar rows (Baird and Lewis 1986). Afferents innervating these rows largely innervate Type B and Type C cells (Baird and Schuff 1994). Moreover, the numbers of Type B and Type C hairs innervated by these afferents are inversely correlated. This suggests that striolar afferents with varying degrees of tonic and phasic gravity sensitivity differ in the number of Type B and Type C hair cells they contact. This hypothesis is supported by the results of the present study, which indicate that Type B cells, whether located in the striolar or extrastriolar region, are sensitive only to low frequencies and are nonadapting or very slowly adapting to hair bundle displacement. Type C cells, on the other hand, rapidly adapt to hair bundle displacement, suggesting that they encode head velocity rather than head position. Type F and Type E cells, which adapt only slowly and to a limited extent, may also contribute to tonic gravity sensitivity. These cells, however, represent only a small percentage of

the total innervation of most striolar afferents (Baird and Schuff 1994).

With the exception of vibratory afferents, utricular afferents in the bullfrog have peripheral innervation patterns (Baird and Schuff 1994) and physiological response properties (Baird and Lewis 1986) similar to those seen in mammals. Recent studies have also shown that the longest stereocilia of Type I and Type II hair cells in mammals display regional variations in morphology similar to those seen in the bullfrog (Lapeyre et al. 1992). Such variations, more subtle than those involved in the separation of hair cells into Type I and Type II varieties, may be associated with differences in hair cell physiology in many vertebrate species, including mammals.

I am indebted to Dr. David C. Corey for a program that predicts tip-link extensions resulting from linear stereociliary displacements. Dr. Robert R. Peterka for a program that estimates, using a least-squares criterion, the parameters of transfer functions to sinusoidal gain and phase data, and to Dr. Miriam D. Burton for assistance with electron microscopy. I am also grateful to N. R. Schuff for figure preparation and assistance during electrophysiological experiments and B. Smith for manuscript preparation.

Funding was provided by National Institute of Deafness and Communicative Disorders Grants DC-00355 and DC-02040, National Aeronautics and Space Administration Grant NCC 2-651, and by grants from the Oregon Lions Sight and Hearing Foundation.

Address for reprint requests: R. A. Baird, R. S. Dow Neurological Sciences Institute, Good Samaritan Hospital and Medical Center, 1120 NW 20th Avenue, Portland, OR 97209.

Received 24 February 1993; accepted in final form 14 October 1993.

REFERENCES

- ANDERSON, D. J., BLANKS, R. H. I., AND PRECHT, W. Response characteristics of semicircular canal and otolith neurons in cat. I. Dynamic responses of primary vestibular fibers. *Exp. Brain Res.* 32: 491-507, 1978.
- ASHMORE, J. F. Frequency tuning in a frog vestibular organ. *Nature Lond.* 304: 536-538, 1983.
- ASSAD, J. A. AND COREY, D. P. An active motor model for adaptation by vertebrate hair cells. *J. Neurosci.* 12: 3291-3309, 1992.
- ASSAD, J. A., HACHOEN, N., AND COREY, D. P. Voltage dependence of adaptation and active bundle movement in bullfrog saccular hair cells. *Proc. Natl. Acad. Sci. USA* 86: 2918-2922, 1989.
- ASSAD, J. A., SHEPHERD, G. M. G., AND COREY, D. P. Tip-link integrity and mechanical transduction in vertebrate hair cells. *Neuron* 7: 985-994, 1991.
- BAIRD, R. A. Morphological and electrophysiological properties of hair cells in the bullfrog utricle. *Ann. NY Acad. Sci.* 656: 12-26, 1992.
- BAIRD, R. A. Comparative transduction and tuning mechanisms of hair cells in the bullfrog utricle. I. Responses to intracellular current. *J. Neurophysiol.* 71: 666-684, 1994.
- BAIRD, R. A., DESMADRYL, G., FERNANDEZ, C., AND GOLDBERG, J. M. The vestibular nerve of the chinchilla. II. Relation between afferent response properties and peripheral innervation patterns in the semicircular canals. *J. Neurophysiol.* 60: 182-203, 1988.
- BAIRD, R. A. AND LEWIS, E. R. Correspondences between afferent innervation patterns and response dynamics in the bullfrog utricle and lagena. *Brain Res.* 369: 48-64, 1986.
- BAIRD, R. A. AND SCHUFF, N. R. Comparative transduction mechanisms of hair cells in the bullfrog utricle. *Soc. Neurosci. Abstr.* 16: 733, 1990.
- BAIRD, R. A. AND SCHUFF, N. R. Transduction mechanisms of hair cells in the bullfrog utricle. *Assoc. Res. Otolaryngol. Abstr.* 14: 38, 1991.
- BAIRD, R. A. AND SCHUFF, N. R. Peripheral innervation patterns of vestibular nerve afferents in the bullfrog utricle. *J. Comp. Neurol.* In press.
- BLANKS, R. H. I. AND PRECHT, W. Functional characterization of primary vestibular afferents in the frog. *Exp. Brain Res.* 25: 369-390, 1976.
- BOYLE, R., CAREY, J. P., AND HIGHSTEIN, S. M. Morphological correlates of response dynamics and efferent stimulation in horizontal semicircular canal afferents of the toadfish, *Opsanus tau*. *J. Neurophysiol.* 66: 1504-1521, 1991.
- CASTON, J., PRECHT, W., AND BLANKS, R. H. I. Response characteristics of

- frog's lagenar afferents to natural stimulation. *J. Comp. Physiol.* 118: 273-289, 1977.
- COREY, D. P. AND HUDSPETH, A. J. Ionic basis of the receptor potential in vertebrate hair cell. *Nature Lond.* 281: 657-677, 1979.
- COREY, D. P. AND HUDSPETH, A. J. Mechanical stimulation and micromanipulation with piezoelectric bimorph elements. *J. Neurosci. Methods* 3: 183-202, 1980.
- COREY, D. P. AND HUDSPETH, A. J. Kinetics of the receptor current in bullfrog saccular hair cells. *J. Neurosci.* 3: 962-976, 1983.
- COREY, D. P., SMITH, W. J., BARRES, B. A., AND KOROSHETZ, W. J. Calmodulin inhibitors block adaptation in vestibular hair cells. *Soc. Neurosci. Abstr.* 13: 538, 1987.
- CRAWFORD, A. C., EVANS, M. G., AND FETTIPLACE, R. Activation and adaptation of transducer currents in turtle hair cells. *J. Physiol. Lond.* 419: 405-434, 1989.
- CRAWFORD, A. C., EVANS, M. G., AND FETTIPLACE, R. The actions of calcium on the mechanoelectric transducer current of turtle hair cells. *J. Physiol. Lond.* 434: 369-398, 1991.
- CRAWFORD, A. C. AND FETTIPLACE, R. An electrical tuning mechanism in turtle cochlear hair cells. *J. Physiol. Lond.* 312: 377-412, 1981.
- DECHESNE, C. J. AND THOMASSET, M. Calbindin (CaBP-28kDa) appearance and distribution during development of the mouse inner ear. *Dev. Brain Res.* 40: 233-242, 1988.
- DECHESNE, C. J., THOMASSET, M., BREHIER, A., AND SANS, A. Calbindin (CaBP 28 kDa) localization in the peripheral vestibular system of various vertebrates. *Hear. Res.* 33: 273-278, 1988.
- DECHESNE, C. J., WINSKY, L., KIM, H. N., GOING, G., VU, T. D., WENTHOLD, R. J., AND JACOBOWITZ, D. M. Identification and ultrastructural localization of a calretinin-like calcium-binding protein (protein 10) in the guinea pig and rat inner ear. *Brain Res.* 560: 139-148, 1991.
- DEMAMES, D., MONIOT, B., LOMRI, N., THOMASSET, M., AND SANS, A. Detection of calbindin-28k mRNA in rat vestibular ganglion neurones by in situ hybridization. *Mol. Brain Res.* 9: 153-156, 1991.
- EATOCK, R. A., COREY, D. P., AND HUDSPETH, A. J. Adaptation of mechanoelectric transduction in hair cells of the bullfrog's sacculus. *J. Neurosci.* 7: 2821-2836, 1987.
- FERNANDEZ, C. AND GOLDBERG, J. M. Physiology of peripheral neurons innervating otolith organs of the squirrel monkey. I. Response to static tilts and to long-duration centrifugal force. *J. Neurophysiol.* 39: 970-984, 1976a.
- FERNANDEZ, C. AND GOLDBERG, J. M. Physiology of peripheral neurons innervating otolith organs of the squirrel monkey. III. Response dynamics. *J. Neurophysiol.* 39: 995-1008, 1976b.
- FUCHS, P. A., NAGAI, T., AND EVANS, M. G. Electrical tuning in hair cells isolated from chick cochlea. *J. Neurosci.* 8: 2460-2467, 1988.
- GILLESPIE, P. G. AND HUDSPETH, A. J. High purity isolation of bullfrog hair bundles and subcellular and topological localization of constituent proteins. *J. Cell Biol.* 112: 625-640, 1991.
- GOLDBERG, J. M., BAIRD, R. A., AND FERNANDEZ, C. Morphophysiological studies of the mammalian vestibular labyrinth. In: *Progress in Clinical and Biological Research. Contemporary Sensory Neurobiology*, edited by M. J. Correia and A. A. Perachio. New York: Liss, 1985, vol. 187, p. 231-245.
- GOLDBERG, J. M., DESMADRYL, G., BAIRD, R. A., AND FERNANDEZ, C. The vestibular nerve in the chinchilla. IV. Discharge properties of utricular afferents. *J. Neurophysiol.* 63: 781-790, 1990a.
- GOLDBERG, J. M., DESMADRYL, G., BAIRD, R. A., AND FERNANDEZ, C. The vestibular nerve in the chinchilla. V. Relation between afferent response properties and peripheral innervation patterns in the utricular macula. *J. Neurophysiol.* 63: 791-804, 1990b.
- HACOHEN, N., ASSAD, J. A., SMITH, W. J., AND COREY, D. P. Regulation of tension on hair-cell transduction channels: displacement and calcium dependence. *J. Neurosci.* 9: 3988-3997, 1989.
- HILLMAN, D. E. AND MCLAREN, J. W. Displacement configuration of semicircular canal cupulae. *Neuroscience* 4: 1989-2000, 1979.
- HOLTON, T. AND HUDSPETH, A. J. The transduction channel of hair cells from the bullfrog characterized by noise analysis. *J. Physiol. Lond.* 375: 195-227, 1986.
- HONRUBIA, V., HOFFMAN, L. F., SITKO, S. T., AND SCHWARTZ, I. R. Anatomical and physiological correlates in bullfrog vestibular nerve. *J. Neurophysiol.* 61: 688-701, 1989.
- HONRUBIA, V., SITKO, S. T., KJMM, J., BETTS, W., AND SCHWARTZ, I. R. Physiological and anatomical characteristics of primary vestibular afferent neurons in the bullfrog. *Int. J. Neurosci.* 15: 197-206, 1981.
- HOWARD, J. AND HUDSPETH, A. J. Mechanical relaxation of the hair bundle mediates adaptation in mechano-electrical transduction by the bullfrog's saccular hair cell. *Proc. Natl. Acad. Sci. USA* 84: 3064-3068, 1987.
- HOWARD, J. AND HUDSPETH, A. J. Compliance of the hair bundle associated with gating of mechano-electrical transduction channels in the bullfrog's saccular hair cell. *Neuron* 1: 189-199, 1988.
- HOWARD, J., ROBERTS, W. M., AND HUDSPETH, A. J. Mechano-electrical transduction by hair cells. *Annu. Rev. Biophys. Biophys. Chem.* 17: 99-124, 1988.
- HUDSPETH, A. J. The cellular basis of hearing: The biophysics of hair cells. *Science Wash. DC* 230: 745-752, 1986.
- HUDSPETH, A. J. AND COREY, D. P. Sensitivity, polarity and conductance change in the response of vertebrate hair cells to controlled mechanical stimuli. *Proc. Natl. Acad. Sci. USA* 74: 2407-2411, 1977.
- HUDSPETH, A. J. AND LEWIS, R. S. Kinetic analysis of voltage- and ion-dependent conductances in saccular hair cells of the bullfrog, *Rana catesbeiana*. *J. Physiol. Lond.* 400: 237-274, 1988.
- LAPEYRE, P., GUILHAUME, A., AND CAZALS, Y. Differences in hair bundles associated with Type I and Type II vestibular hair cells of the guinea pig sacculus. *Acta Otolaryngol. Stockh.* 112: 635-642, 1992.
- LEWIS, E. R., BAIRD, R. A., LEVERENZ, E. L., AND KOYAMA, H. Inner ear: dye injection reveals peripheral origins of specific sensitivities. *Science Wash. DC* 215: 1641-1643, 1982.
- LEWIS, E. R. AND LI, C. W. Hair cell types and distributions in the otolithic and auditory organs of the bullfrog. *Brain Res.* 83: 35-50, 1975.
- LEWIS, R. S. AND HUDSPETH, A. J. Voltage and ion-dependent conductances in solitary vertebrate hair cells. *Nature Lond.* 304: 538-541, 1983.
- LIM, D. J. Morphological and physiological correlates in cochlear and vestibular sensory epithelia. In: *Scanning Electron Microscopy*, edited by O. Johari and R. P. Becker. Chicago: IIT Research Institute, 1976, vol. V, p. 269-276.
- MACADAR, O., WOLFE, G. E., O'LEARY, D. P. AND SEGUNDO, J. P. Response of the elasmobranch utricle to maintained spatial orientation, transitions, and jitter. *Exp. Brain Res.* 22: 1-22, 1975.
- MARTY, A. AND NEHER, E. Tight-seal whole-cell recording. In: *Single Channel Recording*, edited by B. Sakmann and E. Neher. New York: Plenum, 1983, p. 107-122.
- MCLAREN, J. W. AND HILLMAN, D. E. Displacement of the semicircular canal cupula during sinusoidal rotation. *Neuroscience* 4: 2001-2008, 1979.
- MILLER, R. G., JR. Developments in multiple comparisons, 1966-1977. *J. Am. Statist. Assoc.* 72: 779-788, 1977.
- OBERTHOLTZER, J. C., BUETTGER, C., SUMMERS, M. C., AND MATSCHINSKY, F. M. The 28-kDa calbindin-D is a major calcium-binding protein in the basilar papilla of the chick. *Proc. Natl. Acad. Sci. USA* 85: 3387-3390, 1988.
- OHMORI, H. Mechano-electric transducer has discrete conductances in the chick vestibular hair cell. *Proc. Natl. Acad. Sci. USA* 81: 1888-1891, 1984.
- OHMORI, H. Mechano-electric transduction currents in isolated vestibular hair cells of the chick. *J. Physiol. Lond.* 359: 189-217, 1985.
- OHMORI, H. Gating properties of the mechano-electrical transducer channel in the dissociated vestibular hair cell of the chick. *J. Physiol. Lond.* 387: 589-609, 1987.
- OSBORNE, M. P., COMIS, S. D., AND PICKLES, J. O. Further observations on the fine structure of tip links between stereocilia of the guinea pig cochlea. *Hear. Res.* 35: 99-108, 1988.
- PERACHIO, A. A. AND CORREIA, M. J. Responses of semicircular canal and otolith afferents to small angle static head tilts in the gerbil. *Brain Res.* 280: 287-298, 1983.
- PICKLES, J. O., COMIS, S. D., AND OSBORNE, M. P. Cross-links between stereocilia in the guinea-pig organ of Corti, and their possible relation to sensory transduction. *Hear. Res.* 15: 103-112, 1984.
- PITCHFORD, S. AND ASHMORE, J. F. An electrical resonance in hair cells of the amphibian papilla of the frog *Rana temporaria*. *Hear. Res.* 27: 75-84, 1987.
- RABIE, A., THOMASSET, M., AND LEGRAND, C. Immunocytochemical detection of calcium-binding protein in the cochlear and vestibular hair cells of the rat. *Cell Tissue Res.* 233: 691-696, 1983.
- ROBERTS, W. M., HOWARD, J., AND HUDSPETH, A. J. Hair cells: transduction, tuning, and transmission in the inner ear. *Annu. Rev. Cell Biol.* 4: 63-92, 1988.
- RUSSELL, I. J., RICHARDSON, G. P., AND CODY, A. R. Mechanosensitivity

- of mammalian auditory hair cells in vitro. *Nature Lond.* 321: 517-519, 1986.
- RUSSELL, I. J., RICHARDSON, G. P., AND KOSSL, M. The response of cochlear hair cells to tonic displacements of the sensory hair bundle. *Hear. Res.* 43: 55-70, 1989.
- SAIDEL, W. M., PRESSON, J. C., AND CHANG, J. S. S-100 immunoreactivity identifies a subset of hair cells in the utricle and saccule of a fish. *Hear. Res.* 47: 139-146, 1990.
- SANS, A., BREHIER, A., MONIOT, B., AND THOMASSET, M. Immunoelectronmicroscopic localization of 'vitamin D-dependent' calcium-binding protein (CaBP-28k) in the vestibular hair cells of the cat. *Brain Res.* 435: 293-304, 1987.
- SANS, A., ETCHECOPAR, B., BREHIER, A., AND THOMASSET, M. Immunocytochemical detection of vitamin D-dependent calcium-binding protein (CaBP-28K) in vestibular sensory hair cells and vestibular ganglion neurons of the cat. *Brain Res.* 364: 190-194, 1986.
- SEIDEL, R. C. Transfer-function-parameter estimation from frequency response data—a FORTRAN program. *NASA Technical Memorandum.* NASA TM X-3286, 1975.
- SHEPHERD, G. M. G., BARRES, B. A., AND COREY, D. P. Bundle blot purification and initial protein characterization of hair cell stereocilia. *Proc. Natl. Acad. Sci. USA* 86: 4973-4977, 1989.
- SHEPHERD, G. M. G., COREY, D. P., AND BLOCK, S. M. Actin cores of hair-cell stereocilia support myosin motility. *Proc. Natl. Acad. Sci. USA* 87: 8627-8631, 1990.
- THORSON, J. AND BIEDERMAN-THORSON, M. Distributed relaxation processes in sensory adaptation. *Science Wash. DC* 183: 161-172, 1974.
- VIDAL, J., JEANNEROD, M., LIFSCHITZ, W., LEVITAN, H., ROSENBERG, J., AND SEGUNDO, J. P. Static and dynamic properties of gravity-sensitive receptors in the cat vestibular system. *Kybernetik* 9: 205-215, 1971.
- WERSALL, J. AND BAGGER-SJOBACK, D. Morphology of the vestibular sense organs. In: *Handbook of Sensory Physiology. Vestibular System: Basic Mechanisms*, edited by H. H. Kornhuber. New York: Springer-Verlag, 1974, pt. 1, vol. 6, p. 123-170.

